Railway Vehicle Performance Optimisation using Virtual Homologation

Railway Vehicle Performance Optimization Using Virtual Homologation

H. Magalhães[1], **J.F.A. Madeira**[1,2], **J. Ambrósio**[3], **J. Pombo**[1,2,4]

[1]*LAETA, IDMEC, Instituto Superior Técnico, Universidade de Lisboa, Lisboa, Portugal,*

e-mail: hugomagalhaes@tecnico.ulisboa.pt e-mail: jaguilar@dem.ist.utl.pt

[2]*ISEL, IPL, Lisboa, Portugal*

[3]*Instituto Superior Técnico, Universidade de Lisboa, Lisboa, Portugal, e-mail: jorge@dem.ist.utl.pt*

[4]*Heriot-Watt University, Edinburgh, U.K., e-mail: j.c.pombo@hw.ac.uk*

Keywords: Railway Vehicle Acceptance; Multibody Systems; Optimal Performance.

Abstract:

Unlike regular automotive vehicles, which are designed to travel in different types of roads, railway vehicles travel mostly in the same route during their life-cycle. To accept the operation of a railway vehicle in a particular network, a homologation process is required according to local standard regulations. In Europe, the standards EN 14363 and UIC 518, which are used for railway vehicle acceptance, require on-track tests and/or numerical simulations. An important advantage of using virtual homologation is the reduction of the high costs associated to on-track tests by studying the railway vehicle performance in different operation conditions. This work proposes a methodology for the improvement of railway vehicle design with the objective of its operation in selected railway tracks by using optimization. The analyses required for the vehicle improvement are performed under control

of the optimization method Global and Local Optimization using Direct Search (*GLODS*). To quantify the performance of the vehicle, a new objective function is proposed, which includes: a Dynamic Performance Index (*DP*), defined as a weighted sum of the indices obtained from the virtual homologation process; the Non-Compensated Acceleration (*NCA*), which is related to the operational velocity; and a Penalty associated to cases where the vehicle presents an unacceptable dynamic behaviour according to the standards. Thus, the optimization process intends not only to improve the quality of the vehicle in terms of running safety and ride quality, but also to increase the vehicle availability via the reduction of the time for a journey while ensuring its operational acceptance under the standards. The design variables include the suspension characteristics and the operational velocity of the vehicle, which are allowed to vary in an acceptable range of variation. The results of the optimization lead to a global minimum of the objective function in which the suspensions characteristics of the vehicle are optimal for the track, the maximum operational velocity is increased while the safety and ride quality measures of the vehicle, as defined by homologation standards, are either maintained in acceptable values or improved.

Abbreviations

CV – Characteristics values specified in the standards EN 14363 and UIC 518

DP – Dynamic Performance Index

NCA – Non-Compensated Acceleration

GLODS – Global and Local Optimization using Direct Search

PS – Primary Suspension

SS – Secondary Suspension

1. Introduction

The dynamic analysis of multibody models is the primary approach to the study of railway vehicles running on tracks. This is also an important approach for vehicle homologation, as it is was investigated in DynoTrain project [1-3], because it not only allows to reduce the need for experimental tests, thus reducing their approval costs, but also allows to investigate the vehicle dynamics in different conditions, thus providing means to its improvement. In general, the process of homologation of a railway vehicle for a given track, described in international standards [4] requires the assessment of the vehicle dynamics in terms of safety, ride characteristics and track loading. The post-processing of dynamics results required by the virtual homologation leads to the evaluation of Characteristics Values (*CV*), associated to running safety and ride characteristics, which must be within thresholds specified by the standards.

The dynamic analysis of a railway vehicle running in a given track requires the use of three models: vehicle; track and wheel-rail contact force. The accuracy of the models, which is required to use virtual homologation, must be assessed as it is described in the standards, namely, in the section related to model validation [5, 6]. Examples of model validation have been demonstrated in several studies [2, 7, 8]. The vehicle model is characterized by a set of rigid and/or flexible bodies that are interconnected by force elements and joints. Since the flexible modes of the carbody and bogie may be relevant within the frequency range of interest [5, 6], the body structural deformation must be evaluated. It is well known in different modes of transportation that the carbody flexibility has influence on the vehicle ride characteristics [9, 10]. Examples of the vehicle flexibility importance are presented in the literature [11-13], namely, the vehicle-track interaction leads to excitations of the vehicle modes which has impact comfort and fatigue issues. In turn, the representation of the mechanical elements that constrain the relative motion between structural elements is crucial

to preserve representativeness of the model. Springs, dampers, airsprings and actuators are examples of force elements commonly used in railway vehicles. The numerical models of the force elements can be linear or nonlinear, depending on the nature of the element and, eventually, on the range of its application. For example, a helicoidal spring can be represented by a linear spring, however, if it is predictable the contact between coils due to high compress of the helicoidal spring, a bumpstop must be included in the model. A review on modelling of these force elements is presented in the references [14-16]. When modelling kinematic joints, different approaches are available. The most common is to reduce the number of degrees of freedom of the system due to the joint by involving kinematic constraints represented by algebraic equations, which relate independent and depend coordinates of the system. In this case, the reaction forces are computed by the Lagrange multipliers method [17]. A second approach to kinematic joint modelling is by using the contact of clearance joint in which a contact model is imposed. In this case, virtual penetrations between the elements that form the joint and contact laws are used to calculate the reaction forces. Thus, this approach requires additional information, namely, a detailed information of the joint geometry and the parameters for the contact laws [18], being a good alternative to improve the model detail and realism [19].

The railway track model requires the parameterization of its geometry. In the DynoTrain project, this issue motivated the development of a toolkit which is capable, not only to generate test tracks based on measurements of the track geometry, but also to analyse the vehicle response [1]. In this paper, an alternative pre-processor methodology proposed by Pombo and Ambrósio [20] is used. This methodology implemented in a computational pre-processor, which describes fully three-dimensional track and include also the track irregularities, returns one database for each rail in which the position and orientation of the rail is given as function of the rail length. The input for the tool consists in the geometry of the track centreline and

irregularities. Briefly, the track centreline is defined not only by its position, corresponding to the mean value between the left and right rails, but also by the cant, while the irregularities are defined by lateral and vertical deviations of each rail with respect to the track nominal geometry.

The interaction between the vehicle and the track is represented by a wheel rail contact model [21-25]. For studies with focus on the vehicle dynamics, the realism of the contact forces generated in the wheel-rail contact must be assessed as it is described in the standards [5, 6], namely, by comparing the simulated contact forces with the experimental ones which are measured from static and dynamics tests. Moreover, the typical behaviour of wheelsets, namely, the hunting motion in tangent tracks and the flange restriction when the vehicle negotiates curves [26] must be verified. One contact model that accomplishes these demands is proposed by Pombo *et al* [27]. This model follows three steps: firstly, the points of contact, or the points of closest proximity, between wheels and rails are found; secondly, the creepages, i.e., the relative velocities between wheel and rail, are calculated at the points of contact; and, finally, the contact forces are determined, i.e., normal and tangential forces are generated in each contact wheel-rail. Hertzian contact formulation with hysteresis damping is used to find the normal forces [28]. The tangential or creep forces are determined using the formulation proposed by Polach [29]. Of importance to this work is the fact that the wheel-rail interaction forces are calculated by searching the contact conditions online and not via lookup tables. In any case, two potential contact points for each wheel-rail pair are always considered to identify tread-rail and the flange-rail potential contacts. The introduction of the track irregularities is natural in the formulation used here and it does not penalise the contact search algorithm. An example of the application of this contact model is presented in reference [30] where a railway vehicle is simulated in a small curve radius negotiation scenario. Other contact models to represent the wheel-rail interaction have been proposed recently, which account for non-

Hertzian contact conditions [31-35]. These wheel-rail contact models are used in different studies such as the prediction of wear at the wheel-rail interface [36-39], the wheel slip of railway vehicles under degraded adhesion conditions [31-33], and the influence of the plasticity of the wheel-rail on the vehicle behaviour [34, 35].

The acceptance for the operation of a vehicle in a given track via virtual homologation is possible in Europe [4]. The standards EN 14363 and UIC 518 [5, 6], which describe the vehicle homologation process, require that the dynamic response of the vehicle that allows to assess the running safety, ride characteristics and track loading. This data is post-processed using one of the methods prescribed in the standards that fits for the case study. For example, for a vehicle already homologated but subjected to small modifications, such as, the change of the suspension elements, it is applied the Simplified Method defined in the standards. In this case, only the running safety and ride characteristics are assessed. In turn, if the vehicle exhibits new technologies and no background exists, the Normal Method, also described in the standards, is applied, being evaluated not only the running safety and ride characteristics, but also the track loading. In practice, the difference between these methods consists in the quantities that need to be measured. In any of these methods, it is required to post-process the dynamic response of the vehicle, such as, accelerations measured on the vehicle bodies, in order to obtain the *CV*, which in turn must be within the acceptable thresholds prescribed by the standards [5, 6] for the vehicle to be accepted in operation. Modifications of the vehicle characteristics can occur due to the change of its operation condition or in order to improve its dynamic behaviour, for example, the upgrade of a mechanical component may vary the stiffness of the suspension system. In any case, the use of the validated model is possible if the modifications are within the ranges stated in the standards, otherwise, experimental tests are required to verify if the model is still valid.

The use of the *CV* in the virtual homologation process have been demonstrated in several studies. Polach *et al* [7, 40] presented a validation approach where the agreement between *CV* from simulations and those obtained from experimental tests accomplish selected criteria. Suarez *et al* [41-43] investigated the impact on the *CV* when variations of the model parameters are taken into account, namely, the inertial properties of the vehicle structures, the suspension characteristics and the parameters that characterize the wheel-rail contact model. Magalhães *et al* [44] analysed the *CV* obtained from several simulations of a Light Rail Vehicle running in a realistic track with the goal of understanding the impact of the modelling assumptions of the vehicle and the effect of the operational velocity on its acceptance for operation in a metric gauge railway track. More than using the *CV* for virtual homologation they are used in this work as part of the objective function dimmed at the improvement of railway vehicles for optimal operation conditions.

From the point of view of the industry, the optimization procedures play a key role to find the best values of specific mechanical characteristics to improve the performance of a particular system. The formulation of an optimal problem is requires the definition of one or multiple objective functions, the selection of design variables and the definition of appropriate constraints [45]. In several engineering applications, the objective functions may not be defined by explicit equations, but, instead, be evaluated computationally by performing simulations of the system dynamics. One example of the application of this type of approach is presented by Gonçalves and Ambrósio [10] in the framework of road vehicle dynamics, being the suspension characteristics of a road vehicle optimized in order to improve the comfort perceived by the passengers. The optimization tool developed simulates the vehicle in a variety of scenarios being the accelerations obtained processed to obtain comfort indexes and, consequently, to quantify the objective function that allows the vehicle improvement. The problem posed by the optimization of the railway vehicle for its virtual homologation, fulfilling the standards [5, 6], is

that several conflicting objectives may be identified, in particular the *CV* associated to running safety and ride characteristics and the operational velocity. Therefore, the problem must be formulated within the framework of multiple objective optimization [46]. In this case, instead of a single solution the optimization procedure identifies a set of solutions, deemed as Edgeworth-Pareto optimal solutions or Pareto Front, for which no better solution for a particular objective can be achieved without worsening another objective [47]. Afterwards, the solution selected among those of the Pareto front, requires some form of engineering decision. Another approach to handle multiobjective optimization problems is to solve a single objective optimization problem while keeping the current values of the remaining objectives as unilateral constraints of the problem. This approach is demonstrated by Gonçalves and Ambrosio [9] in the optimization of a road vehicle suspension for both ride quality and running safety optimization in which a sequence of optimal problems is solved by alternating the ride quality and the running safety functions as objective functions and unilateral constraints. A third approach is to reduce the multiobjective optimization problem to a single optimization problem by forming the objective function as a weighted sum of all objectives [48]. This approach requires a prior decisions on the weight of each objective function, which requires some engineering knowledge of the system under analysis [46].

When formulating the problem as a multiple objective optimization, its solution, i.e., the identification of the Pareto Front, is obtained by using an evolutionary optimization method [49], among which the genetic algorithms [50], simulated annealing [51], swarm optimization [52], and others, are possible choices. When formulating the problem as a single objective function, either due to the use of one of the approaches to handle a multiple optimization problem or because the problem is single objective in the first place, the use of gradient based optimization methods [46] and of evolutionary algorithms must be defined based on the characteristics of the problem to solve. When the optimization problems are characterized by a

large number of minima, noisy responses or discontinuous feasible spaces the use of deterministic optimization methods often lead to solutions associated to local minima. The search for the best minimum of the objective function can be done by solving a more or less large number of optimization problems with different initial conditions, generated using an approach algorithm for the design of experiments [53, 54]. In any case, the number of system analysis that is required to obtain a good minimum, not necessarily the global minimum, may become very large when using this strategy.

The use of non-deterministic optimization methods in the context of the problem addressed in this work, for which not only the design space is not convex, but also there is no assurance that it is continuous while the system response is noisy, is preferred to allow the identification of a global minimum. The *GLODS* method developed by Custódio et al [55] is selected among other derivative-free algorithms due to its good performance in the identification of the best regions of the design space to be searched for the best minimum. The strategy to reduce the multiple objective optimization problem to a single objective function resulting from the weighted sum of the individual objective functions is used in the formulation of the problem.

The main purpose of this work is to present a methodology to improve the quality of a railway vehicle in terms of its running safety and ride characteristics while allowing for the reduction of its journey time in the selected tracks where it is supposed to operate mostly. The vehicle is represented by a multibody model characterized by a set of bodies interconnected by spring-damper elements [44, 56, 57]. Even though the standards specify requirements related to track extension and the consideration of track irregularities, in this work, the track used for optimization is selected among the segments of the complete railway track considering the worst *CV* obtained from preliminary studies. Here, the topology of the track is chosen in order to define a case where the vehicle optimization is important and, in turn, the

extension of the track is defined in order to obtain reliable values of *CV*. A proper objective function to accomplish the objectives of the optimization, which combines the definition of a novel Dynamic Performance Index with the operational velocity of the vehicle and with the penalization of the violation of any safety or ride quality threshold, is proposed in this work. The selection of the design variables is based, not only on easy and economical modification of existing vehicles, but also on their impact to the vehicle dynamics [41-43, 58]. The optimization tool developed here runs successive dynamic analysis in batch mode, i.e., without requiring any manual intervention from the user, under control of the Global and Local Optimization using Direct Search method in order to identify an optimal vehicle design. The optimization results obtained with this approach effectively demonstrate that not only by small adjustment of the vehicle suspension a better performance is obtained, both in terms of running and ride characteristics, but also higher operation velocities can be used while fulfilling all acceptance criteria enforced by the standards EN 14363 and UIC 518. From the optimization results, it is suggested what changes must be applied, namely what the characteristics of the suspension systems must be used, and what is the maximum operational velocity of the railway vehicle. Note that the feasibility of such changes is quantified as lower and upper bounds of the design variables and, if fulfilled, are always ensured.

2. Multibody Formulation

The dynamic analysis of a multibody system involves the study of its motion and of the internal and external forces developed during a time period. A generic multibody model, as shown in Figure 1, is defined by a collection of rigid and/or flexible bodies interconnected by kinematic joints and/or force elements. The kinematic joints constrain the relative motion between the bodies, while the force elements represent the internal forces that develop between bodies due to their relative motion. External forces, as those resulting from the interaction with the surrounding environment such as those that develop due to wheel-rail

contact, may also be applied to the system components. Both internal and external forces are described by using suitable constitutive relations between kinematic quantities such as springs, dampers or contact elements.

When using Cartesian coordinates, the equations of motion for a multibody system are written together with the second time derivative of constraint equations as [17]:

$$\begin{bmatrix} \mathbf{M} & \mathbf{\Phi}_q^T \\ \mathbf{\Phi}_q & \mathbf{0} \end{bmatrix} \begin{Bmatrix} \ddot{\mathbf{q}} \\ \boldsymbol{\lambda} \end{Bmatrix} = \begin{Bmatrix} \mathbf{f} \\ \boldsymbol{\gamma} \end{Bmatrix} \tag{1}$$

where $\mathbf{M}$ is the mass matrix, $\ddot{\mathbf{q}}$ is the vector of the system accelerations, $\mathbf{f}$ is the force vector, $\mathbf{\Phi}_q$ is the Jacobian matrix associated to the kinematic constraints, $\boldsymbol{\lambda}$ is the vector of Lagrange multipliers, which are related to the joint reaction forces, and $\boldsymbol{\gamma}$ is the right-hand side of the acceleration constraint equations. The solution of the forward dynamics problem is obtained by using a variable time step and variable order numerical integrator [59].

2.1 Multibody Model of a Railway Vehicle

The railway vehicle is based on an existing light rail vehicle being all data realistic, but it is altered due to the need to preserve confidentiality. Therefore, the geometrical, inertial and suspension force elements data used here is based on the model published by Magalhães et al [44] in order to preserve the realism of the railway vehicle model.

This model is composed by one carbody, two bogie frames and four wheelsets as shown in Figure 2. The primary suspension, i.e., the elements that interconnect the wheelsets and the bogies frames, and the secondary suspension, i.e., the elements that interconnect the bogie frames and the carbody, are modelled by sets of spring and damper placed in parallel, as shown in Figure 2. The centre of gravity (*CG*) of the bodies and their mass properties are listed in Table 1. Table 2 lists not only the dynamic characteristics of the force elements, namely, the stiffness, k, the damping, c, and the undeformed length, L_0, but also their

attaching points P_i and P_j, as shown in Figure 2 by small circles. Note that only the right hand side of the primary and secondary suspension is described. The suspension of each bogie is symmetric and the information on the remaining elements can be obtained taking into account the vehicle symmetry, namely, the longitudinal plane *XZ*.

2.2. Track Model

The track model is represented by two parametric surfaces that result from extruding of the rail profile along two paths, the left and right rails. The parameters necessary to describe the track geometry in nominal conditions or considering track irregularities are introduced at this stage, i.e., during the sweep of the rail profile of the rail centrelines. The rail profile considered in this work is the UIC 54 [60].

A railway track can be split into three types of sections: tangents, curve transitions and curves. Curve transitions are present between tangents and curves, as shown in Figure 3. To define the track geometry, four parameters, function of the track length, are required:

- the gauge, *G*, which is the distance between the inner edges of the rails heads;
- the instantaneous radius, *R* of the track;
- the cant angle, φ, which is the track inclination with respect to the horizontal plane;
- the rail cant, β, which is the rail inclination with respect to the track plane.

The parameters *G*, φ and β are depicted in Figure 4. In nominal conditions, *G* and β are constant, while the curvature, i.e., the inverse of *R*, and φ varies with the track length, being constant in tangent and curve segments and varying linearly in curve transition segments, as shown in Figure 3.

In reality the track geometry changes over the years due to its usage thus leading to irregularities. The simplest way to describe the irregularities of the track is by considering the lateral, *LD*, and vertical, *VD*, deviations with respect to the nominal geometry, being the

deviations related to the left and right rail assessed independently. Figure 5 shows (a) a rail in nominal conditions, (b) a rail characterized by a lateral deviation and (c) a rail characterized by a vertical deviation. Further information on track geometry can be found in [20]. Note that in practice, the irregularities are only obtained by experimental measurements, although in some special cases they can be generated numerically.

2.3. Wheel-Rail Contact Model

The interaction between the vehicle and the track is represented by a contact model. The contact model used in this work considers two potential contact points, the tread-rail and the flange-rail contacts, as shown in Figure 6. The wheel profile is defined by two sets of nodal points, one for the tread and the other for the flange profile. These nodal points are interpolated in order to define the cross section of the profile. The rail profile is obtained by the interpolation of a set of nodal points. The wheel and rail parametric surfaces result from the revolute sweep and of the translational sweep of the respective cross sections, as shown in Figure 6.

During the dynamic analysis, the two possible contacts are assessed on-line during the dynamic analysis. For each of potential contact point such as those shown in Figure 7, a non-linear system of equations needs to be solved. The minimal distance between two surfaces is defined by:

$$\begin{aligned} \mathbf{d}\times\mathbf{n}_i = \mathbf{0} \equiv \begin{cases} \mathbf{d}^T\mathbf{t}_i^u = 0 \\ \mathbf{d}^T\mathbf{t}_i^w = 0 \end{cases} \\ \mathbf{d}\times\mathbf{n}_j = \mathbf{0} \equiv \begin{cases} \mathbf{d}^T\mathbf{t}_j^s = 0 \\ \mathbf{d}^T\mathbf{t}_j^t = 0 \end{cases} \end{aligned} \tag{2}$$

where $\mathbf{d}$ is the distance vector between the potential points of contact, $\mathbf{n}_i$ and $\mathbf{n}_j$ are the normal vector of surfaces *i* and *j*, $\mathbf{t}_i^u$ and $\mathbf{t}_i^w$ are tangential vectors of surface *i* and $\mathbf{t}_j^s$ and $\mathbf{t}_j^t$ are

tangential vectors of surface *j*, as shown in Figure 7. For each contact pair, two cases can occur, the existence or not existence of virtual indentations. The contact exists if:

$$\mathbf{d}^T\mathbf{n} > 0 \tag{3}$$

In case of contact, normal and tangential forces are generated. These forces depends not only on the contact conditions, but also on the mechanical properties associated to the wheel and rail. Here, the Hertz contact force model with hysteresis damping is used to compute the normal forces written as:

$$f_n = K\left(1+\frac{3\left(1-e^2\right)}{4}\frac{\dot{\delta}}{\dot{\delta}^{(-)}}\right)\delta^n \tag{4}$$

where *K* is the stiffness coefficient, *e* is the restitution coefficient, *n* is a constant equal to 1.5 for metals, δ is the amount of indentation between the surfaces, $\dot{\delta}$ is the indentation velocity and $\dot{\delta}^{(-)}$ is the relative velocity before the impact. For the tangential forces, the formulation proposed by Polach is used [29]. Besides the simplifications used, this model takes into account the spin effect and its computational efficiency is better than others approaches, such as, the Kalker linear theory [61] or the heuristic non-linear model [62]. The detailed description of the formulation of the wheel-rail contact is presented in the reference [56].

3. Railway Dynamics

3.1 Virtual Homologation

Multibody simulation programs are used to represent realistic simulations of railway vehicles running in selected tracks. The vehicle dynamic response, obtained either as result of experimental or virtual testing, is required by the standards, namely, the accelerations of the carbody and bogie frames and the forces developed at the wheel-rail contacts [4]. To assess the dynamic behaviour of the vehicle from the safety and ride quality point of view, several

performance indexes are required, as described in the standards [5, 6]. A simple example of the application of this procedure is well detailed in reference [44].

Depending on the homologation case, two different methods can be applied. The Normal Method is used for the homologation of vehicles that have not been homologated before or when subjected to large modifications. For vehicles already homologated but subjected to minor modifications, at most, are homologated using the Simplified Method, as described in the standards [5, 6]. Without loss of generality, and to overcome confidentiality reasons, the vehicle model used here is based on a real existing vehicle already homologated for operation on various railway tracks. In this sense, the already homologated vehicle is subjected to slight modifications, being the Simplified Method applicable. This method requires the evaluation of the following quantities: lateral acceleration measured on the bogie frames above of the outer wheelsets, $\ddot{y}^{+}$; lateral and vertical acceleration, respectively, measured on the carbody above the bogies, $\ddot{y}^{*}$ and $\ddot{z}^{*}$. The relative position of measurement points with respect to local reference frame of the body is shown in Figure 8 by black dots. The outer wheelsets are also indicated in Figure 8.

The dynamic response of the vehicle is obtained with a reporting frequency of 200 Hz, which is the minimum accepted in the standards. According to the Simplified Method, the specifications for the filters, statistical quantities and constant *K* to be applied to each dynamic response are listed in Table 3. In this post-processing, the statistical quantities are obtained from the cumulative distribution curves and root mean squares. The values F_1, F_2 and F_0 are the frequency of the cumulative distribution curve.

3.2 Non-Compensated Acceleration

The Non-Compensated Acceleration [63] is defined by a relation between the centrifugal and gravitational accelerations applied on the carbody in its local lateral direction. The *NCA*, depicted in Figure 9, is obtained by:

$$NCA = a_{c,\varphi} - a_g = \frac{V^2}{R}\cos(\varphi) - g\sin(\varphi) \tag{5}$$

where $a_{c,\varphi}$ is the local lateral acceleration of the carbody due to the centrifugal acceleration a_c, V is the velocity of the vehicle, R is the radius of the curve, φ is the cant angle, as depicted in Figure 9, and g is the gravitational acceleration (9.81 m/s^2). The velocity as function of the *NCA* is defined as:

$$V\left(NCA\right) = \sqrt{\frac{R\left(NCA + g\sin(\varphi)\right)}{\cos(\varphi)}} \tag{6}$$

The operation velocity is designed based, not only on the geometry of track, namely, the curve radii and cant angles, but also on the *NCA*. To achieve optimal comfort of the passengers, the velocity must be defined such that the *NCA* is null, i.e., *NCA*=0 m/s^2. Minor variations of the operation velocity are possible, however, the range of admissible values of *NCA*, namely, 0<|*NCA*|<1 m/s^2, must be ensured [63]. In turn, according to the standards [5, 6], the speed in curve segments is constrained based on the cant deficiency, namely, the speed must be set such that the cant deficiency applied is within the range of 0.75-1.1 of the maximum cant deficiency allowed for a given vehicle. For example, in case of the European gauge passenger vehicles, the maximum cant deficiency allowed is 150mm, i.e., the outer rail should be lifted 150 mm in order to cancel *NCA*. The correspondent range in terms of *NCA* is 0.78-1.15m/s2. Thus, the constraint used, namely, 0<|*NCA*|<1 m/s2, does not exceed the limits imposed in the standards and it allows to check if the vehicle can reach, at least, the range imposed in the standards.

4. Preliminary Studies for Track and Model Parameter Selection

4.1 Track Operating Scenarios

Firstly, the vehicle is tested in six different railway tracks. The *CV* are obtained for each simulation. From these results, the worst scenario that can benefit from a redesign of the vehicle suspension is identified. The topology of the tracks is characterized by the sequence of segments: tangent (50 m); curve transition (25 m); curve (100 m); curve transition (25 m) and tangent (50 m). Thus, all tracks have 250 meters of extension as shown in Figure 3. The differences between the tracks resides on the curve radius, which is 1000 m for 'T1' and 'T4', 500 m for 'T2' and 'T5', and 200 m for 'T3' and 'T6', and on the existence of track irregularities in the tracks used for cases 'T4', 'T5' and 'T6'. These irregularities were measured experimentally in one curved track of the Lisbon subway railway network. Figure 10 shows the lateral, *LD*, and vertical, *VD*, deviation of the left and right rails, which are schematically depicted in Figure 5. It must be noticed that the first tangent segment is used to place the vehicle model in contact with the track model and to start the simulation. Therefore, not only no irregularities are used in this first tangent segment but also the vehicle dynamic response, while in this segment, is not used for any purpose. The nominal cant angle of the curve segment for both track types is 5 degrees. The speed considered in each simulation is defined such that the *NCA* is equal to 0.5 m/s^2. Table 4 summarizes the scenarios considered here.

The *CV* related to running safety and to ride characteristics, for each one of the scenarios considered, are presented in Figure 11 and Figure 12, respectively. In this case the *CV* are evaluated for the tangent segments and for the curve segments, separately, being the *CV* presented as a percentage of the limits specified in the standards [5, 6]. These results suggest that when the radius of the curve segment is increased and track irregularities are introduced, the *CV* tend to increase. It is also observed that *CV* related to lateral accelerations on the carbody for curve segments are closer to the limits than what is observed for tangent segments.

Two criteria are used to select the case study which can benefit from the optimization procedures. First, the simulations with higher *CV*, which represent the worst case studies for vehicle acceptance are to be considered, i.e., the scenarios ‘T1’ and ‘T4’ are selected. Second, because only the work now presented intends to demonstrate a design methodology, the simulation cost is used here to select the demonstrative scenario. With this reasoning in mind ‘T1’, which is approximately 1.6 times faster to simulate than ‘T4’ due to lack of irregularities, is the scenario selected here to demonstrate a feasible methodology for the improvement of railway vehicles. Note that in the application of the methodology proposed here to a real industrial application, the track irregularities information must be included in the track model.

4.2 Track Length

The complete railway track in which the operation of the railway vehicle running is considered is composed by a series of 30 sections, S1, S2,… S30, depicted in Figure 13. Each section represents the track ‘T1’, described in Table 4.

The variation of *CV* as function of the number of sections of the complete track is first considered in order to identify the minimal track length in which to develop the virtual testing. The *CV* related to running safety for tangent and curve segments, denoted by CV^t and CV^c, respectively, are shown in Figure 14 and Figure 15. It is observed, for all cases, that the *CV* are well stabilized after 1000 meters of track.

The variation of *CV* related to ride characteristics are more sensitive to the track length as shown in Figure 16 for tangent segments and in Figure 17 for curve segments. It is observed that the *CV* start stabilizing after 2000 meters which correspond to 8 sections of track with the characteristics of segment ‘T1’. Thus, the railway track used for the optimization study consists in a serie of 8 segments of the track considered in simulation ‘T1’.

4.3 Dynamic Performance Index

A suitable objective function for the optimal problem that can take into account the contribution of the *CV* defined in the standards is required. A Dynamic Performance Index (*DP*) is proposed here to quantify the performance of the railway vehicle in the selected track, defined in the previous section, and involving all safety and ride quality *CV*. For this purpose, let the weighted sum of a running safety index WS_{rs}, and of a ride quality index, WS_{rc}, be written as:

$$DP = \alpha WS_{rs} + (1-\alpha) WS_{rc} \tag{7}$$

where $0<\alpha<1$ is a constant set by the user that weights the relative importance between running safety and ride characteristics. In this study, running safety is deemed as more important that ride quality and $\alpha=0.7$. The running safety index, WS_{rs}, and the ride quality index, WS_{rc}, are defined as a weighted sum of the same indexes defined for tangent track and

$$WS_{rs} = \beta WS_{rs}^{t} + (1-\beta) WS_{rs}^{c} \tag{8}$$

$$WS_{rc} = \beta WS_{rc}^{t} + (1-\beta) WS_{rc}^{c} \tag{9}$$

for curved track as:

where $0<\beta<1$. The superscript *t* refers to tangent track and *c* to the curve track while the subscripts *rs* continues to refer to running safety and *rc* to ride characteristics. In order to penalize any reduction of the safety or ride quality in curves the value of $\beta=0.3$ is used hereafter.

The running safety and the ride quality indexes for the tangent and curve track are now defined as weighting sums of the *CV* defined in Table 3. By defining $i=1,\ldots,6$ as the counter of the *CV* for running safety and $i=7,\ldots,16$ as the counter of the *CV* for ride quality while $j=1$ refers to tangent track and $j=2$ refers to curve track, the following weighted sums are defined:

$$WS_{rs}^{t} = \sum_{i=1}^{6} w_{i,j} CV_{i,j}, j = 1$$

$$WS_{rs}^{c} = \sum_{i=1}^{6} w_{i,j} CV_{i,j}, j = 2$$

$$WS_{c}^{t} = \sum_{i=7}^{16} w_{i,j} CV_{i,j}, j = 1 \quad (10)$$

$$WS_{c}^{c} = \sum_{i=7}^{16} w_{i,j} CV_{i,j}, j = 2$$

The weights $w_{i,j}$ are calculated here using the $CV_{i,j}$ obtained for the initial model of the railway vehicle running in the test track and take into account the limit $CV_{i,j}^{\lim}$ of each one of them. The weights that effectively penalize more the $CV_{i,j}$ closer to their limits, are evaluated as:

$$w_{i,j} = \frac{CV_{i,j}}{CV_{i,j}^{lim}} \sum_{k=1}^{6} \left(CV_{k,j} \Big/ CV_{k,j}^{lim} \right)^{-1}, i = 1,2,...,6; j = 1,2$$

$$w_{i,j} = \frac{CV_{i,j}}{CV_{i,j}^{lim}} \sum_{k=7}^{16} \left(CV_{k,j} \Big/ CV_{k,j}^{lim} \right)^{-1}, i = 7,8,...,16; j = 1,2 \quad (11)$$

The definition of the $CV_{i,j}$ is summarized in Table 5 as well as the weights $w_{i,j}$ obtained for the original vehicle in the test track using equation (11). It must also be noted that the sums of the weights for running safety and for ride characteristics for tangent and curve tracks must be unitary, i.e., $\sum_{i=1}^{6} w_{i,j} = 1$ and $\sum_{i=7}^{16} w_{i,j} = 1$ for j=1,2.

4.4 Selection of the Design Variables

The optimization of the railway vehicle to run in the track is achieved by fitting the primary and the secondary suspension to improve the Dynamic Performance Index. Table 6 lists the potential design variables that include not only the stiffness, *k*, and damping, *c*, of the primary suspension (*PS*), and of the secondary suspension (*SS*), but also the *NCA*. The lower

and upper bounds of the domain of interest for each potential design variable is also presented in Table 6. The arbitrary factor χ is considered to be equal to 0.1 in order to include a large range of values for the design variables related to the suspension characteristics. In a real application this large modification would require experimental tests to verify that the optimal model provides validated results.

The selection of the design variables to be used in the optimization, among those listed in Table 6, is done by performing a sensitivity analysis in which the variation of *DP* is computed with respect to the variation of each one of the potential design variables. To perform this sensitivity analysis let the non-dimensional variables be defined as:

$$x_k = \frac{v_k^0 - v_k^{lower}}{v_k^{upper} - v_k^{lower}}, k = 1,...,13 \tag{12}$$

where v_k^0, v_k^{lower} and v_k^{upper} are the quantities in Table 6, for instance k=7 refers to the longitudinal stiffness of the secondary suspension being $v_7^0 \equiv k_{SS,long}^0$, $v_7^{lower} \equiv \chi k_{SS,long}^0$ and $v_7^{upper} \equiv (1-\chi) k_{SS,long}^0$.

Each potential design variable x_k, k=1,…,3 takes the values 0.40, 0.45, 0.50, 0.55 and 0.60 in each one of the virtual tests. The variation of *DP* for each variable x_k is generically shown in Figure 18. The maximum variation of *DP* for each variable x_k, defined as $\Delta DP(x_i)$, is identified and plotted in Figure 19 as a percentage with respect to the highest value observed in all virtual tests.

By observation of Figure 19 the parameters of the vehicle suspension model to which *DP* is more sensitive are the primary suspension longitudinal and lateral stiffness, $K_{PS,long}$ and $K_{PS,lat}$, and the lateral stiffness of the secondary suspension $K_{SS,lat}$. Besides the obvious choice of these parameters as design variables also the *NCA* is selected as design variable due to the fact that it is the only variable that allows modifying the operational velocity if the vehicle.

5 Optimal Design of the Vehicle Suspension and Operation Speed

5.1 Formulation of the Optimal Problem

One goal of this work is to maximize the operation velocity of the vehicle keeping the *CV* values lower than the limits specified in the standards [5, 6] so that it can be homologated for operation in the selected track. Generically, the optimization problem is defined as:

$$\begin{aligned} &\min f(\mathbf{x}) \\ &s.t. g_{i,j}(\mathbf{x}) \le 0 \\ &\mathbf{x}^{lower} \le \mathbf{x} \le \mathbf{x}^{upper} \end{aligned} \tag{13}$$

For the optimization of the railway vehicle the design variable vector $\mathbf{x}=[x_1, x_2, x_3, x_4]^T$ is composed of the model suspension parameters identified in the previous section and listed in Table 7. The restrictions of the optimal problem are the limit values of the *CV* that still warrant the vehicle approval, written as:

$$g_{i,j}(\mathbf{x}) \le CV_{i,j}^{\lim}, i = 1,2,...,16; j = 1,2 \tag{14}$$

The objective function to be minimized includes the Dynamic Performance Index and a measure of the operation velocity. The objective function used in this optimal problem is defined as:

$$f(\mathbf{x}) = \mu DP(\mathbf{x}) - (1-\mu) NCA(\mathbf{x}) + P(\mathbf{x})C \tag{15}$$

where the minimization of the function corresponds to a minimization of the Dynamic Performance index, $DP(\mathbf{x})$, a maximization of the $NCA(\mathbf{x})$ and a minimization of the violation of the problem restrictions, represented by $P(\mathbf{x})$. In this objective function Non-Compensated Acceleration $NCA(\mathbf{x})$ is used as a measure of the operation velocity due to the proportionality between these quantities. The parameter μ=0.5 is selected to give the same weight to the terms $DP(\mathbf{x})$ and $NCA(\mathbf{x})$ in the optimal problem. The term $P(\mathbf{x})$ effectively introduces the restriction $g_{i,j}(\mathbf{x})\le 0$ violation in the objective function as:

$$P(\mathbf{x}) = \left(\sum_{j=1}^{2} \sum_{i=1}^{16} \max\left(0, \frac{CV_{i,j}}{CV_{i,j}^{\lim}} - 1\right) \right)^2 \tag{16}$$

Therefore, by using $P(\mathbf{x})$ in the objective function, the side constraints $g_{i,j}(\mathbf{x})$, appearing in equation (13), are not necessary in the standard formulation of the optimal problem. The weight of the penalization of the restrictions violations is defined as:

$$C = \frac{V_{\max}}{V\left(NCA(\mathbf{x})\right)} \tag{17}$$

where $V(NCA(\mathbf{x}))$ is the velocity of the vehicle and V_{max} is the maximum possible velocity of the vehicle corresponding to NCA=1m/s^2. Consider two given designs, $\boldsymbol{x}_1$ and $\boldsymbol{x}_2$, for which the respective penalty function are approximately equal, i.e., $P(\mathbf{x}_1) \approx P(\mathbf{x}_2)$. Suppose now that the velocity of $\mathbf{x}_1$ is higher than $\mathbf{x}_2$, i.e., $V(NCA_1) > V(NCA_2)$. In practice, the point $\mathbf{x}_1$ is better than $\mathbf{x}_2$. Therefore, the weighting factor C effectively divides $P(\mathbf{x})$ by the velocity $V(NCA)$, while the multiplication by the maximum velocity that the vehicle can achieve, V_{max}, normalizes it and makes it non-dimensional.

One particular aspect of the formulation of the optimal problem concerns derailment being the penalization of this event heavily emphasized. One way to detect the derailment would be the assessment of Y/Q ratio, i.e., the ratio between the lateral and vertical forces developed in the wheel-rail contact, however, from the computational point of view, derailment can be detected either by a null normal contact force in any of the rail-wheel contact pairs or by the impossibility to conclude a virtual test, usually associated to a premature termination of the simulation. Defining the group of feasible design variables by S, i.e., the group of vectors $\mathbf{x}$ for which no derailment is identified, the definition of $P(\mathbf{x})$ and $DP(\mathbf{x})$ is now modified as:

$$P(\mathbf{x}) = \begin{cases} P(\mathbf{x}) & \text{if} \quad \mathbf{x} \in S \\ +\infty & \text{if} \quad \mathbf{x} \notin S \end{cases} \tag{18}$$

$$DP(\mathbf{x}) = \begin{cases} DP(\mathbf{x}) & \text{if} \quad \mathbf{x} \in S \\ +\infty & \text{if} \quad \mathbf{x} \notin S \end{cases}$$

In practice, anytime derailment is detected the objective function reaches a maximum.

The definition of the optimization problem that involves the objective function defined in equation (15) effectively involves the constraints via the term $P(\mathbf{x})$. Therefore, the optimal problem originally specified in equation (13) is now re-written as an unconstrained optimal problem defined as:

$$\min_{s.t.\mathbf{x}\in\boldsymbol{\Omega}} f(\mathbf{x}) \tag{19}$$

where $\boldsymbol{\Omega}$ is the feasible domain of the design variables $\mathbf{x}$ defined by the upper and lower bounds listed in Table 7. The optimal problem defined in the form of equation (19) is now suitable to be used with non-deterministic optimization algorithms, such as the global optimization method considered hereafter.

5.2 Optimization Method

The solution of the optimization problem posed by equation (19) is achieved here by using the Global and Local Optimization with Direct Search [55]. *GLODS* is a new algorithm for single optimization, suited for bound constrained, derivative-free and global optimization. Using direct-search of directional type, the method alternates between a search step, where potentially good regions are located, and a poll step where the previously located regions are explored. This exploitation is made through the launching of several pattern search methods, one in each of the regions of interest. Differently from a multistart strategy, the several pattern search methods merge when sufficiently close to each other. The goal of *GLODS* is to end with as many active pattern searches as the number of local minimizers, which would allow to easily locating the possible global extreme value.

The *GLODS* is chosen to solve the optimization problem for three reasons: first, because there is no explicit equation of the objective functions; second, taking into account that each evaluation of the cost function requires a simulation that takes approximately one hour, this method is preferable to others, such as, evolutionary methods that require many evaluations to generate new populations; and, finally, because it is a global optimization method.

Another important characteristic of this method is related to the strategies used to exploit the domain. The *GLODS* alternates between a search and a poll step. In the search step, starting points are generated according to a given strategy, being used in this work the 2^n-centre strategy. This strategy starts by enclosing the feasible region in a box, which is going to be consecutively subdivided into smaller boxes, defining different levels of searches. At each level, the points to be selected for evaluating the objective function correspond to the box centres. Note that by point it is meant a set of design variables. Figure 20 exemplifies the procedure for a bound constrained problem of dimension n=2. An exception occurs at level 0, case (a), where all the vertices of the box are additionally considered.

Once the starting points are defined, the poll step is performed. Consider one starting point represented in Figure 21 in grey of step i. The poll method determines points in the neighbourhood according to a positive spanning set which are represented by black points in Figure 21. After the evaluation of the cost function of these points, they are compared and two cases can occur: there is success, i.e., at least, one point of the neighbourhood is better than the others; there is no success, i.e., the initial point is better than the neighbourhood points. In case of success, the best point is the initial point of the step i+1 and the mesh size could be increased or kept equal, as shown in Figure 21 (a) and (b). Otherwise, the initial point for the step i+1 is the same and the mesh size is reduced, as depicted in Figure 21 (c). When the poll method related to each starting point converges, new starting points are generated for the next iteration. In this way, different minima of objective functions can be determined.

5.3 Optimization Results

The cost functions for 431 points, resulting from the evaluating of the objective function during two weeks, as required by the methodology, in a standard desktop computer with an Intel i7 processor, are shown in Figure 22. These points are sorted in ascending order of the objective function and not in the order of their occurrence for display purposes only. Among the points evaluated, 14 of them are related to cases where the simulations are not admissible and, consequently, the cost function is $+\infty$. Considering the 250 best points, as shown in the bottom graph of Figure 22, the cost function never exceed 4.0 because, in these cases, the penalty term $P(\mathbf{x})$, defined in equation (16), is null or small. The cost functions associated to the other points are high, reaching the order of magnitude of 10^3, due to the violation of the restrictions imposed in the standards.

Figure 23 presents the design variables values of the 100 best points, being ordered according the presentation of the objective functions in Figure 22. A good convergence of the design variables is identified taking into account their small variation when only the first 10 objective functions are considered. This suggests that this optimization problem is characterized by one global minimum with the vector of design variables written as $\mathbf{x}^*=[1.893, 0.325, 1.163, 0.625]^T$.

Table 8 summarizes the design variables, for three designs: the Initial case corresponds to the centre of the design variables domain; the Optimal case corresponds to design variables for which the vehicle leads to the lower value of the cost function $f(\mathbf{x})$; and, the Original case is characterized by the vehicle suspension parameters measured in the currently existing vehicle. The parameters listed include the design variables, operation velocity and cost function. Regarding the suspension characteristics, an increase of $k_{PS,long}$ and a reduction of $k_{PS,lat}$ is suggested, while $k_{SS,lat}$ is recommended to be slightly increased. It is of special interest to notice the increase of the operation velocity from the Original to the Optimal case, i.e., an

increase of 9.25 m/s (or 33.3 km/h) is possible while fulfilling the homologation criteria, which potentiates a significant reduction of journey time without running on the limits of *CV*.

6 Conclusions

An optimization approach for design the suspension characteristics and the definition of the operation velocity of a railway vehicle that improves its dynamic behavior for a given track while fulfilling the appropriate homologation standards [5, 6], was proposed here. The optimal problem is formulated being the objective function defined as a sum of three terms: Dynamic Performance Index, which is a new measure of performance proposed here; Non-Compensated Acceleration, which is directly related to the operation velocity; and a Penalty function, which not only penalizes the violation of the Characteristic Values according to the limits established by the standards but also includes events of vehicle derailment. The topology of the track is selected considering the worst behavior of the railway vehicle, according to the *CV*. The track extension is defined based on a compromise between two aspects: it must be as short as possible in order to avoid long simulations; each simulation must be long enough to provide reliable evaluations of the *CV*. The Dynamic Performance Index is defined here and proposed as a lumped representation of the *CV* considered in the standards. The simulation, in a batch mode, which offers a high potential for the parallelization of the simulations, is controlled by the Global and Local Optimization procedure using Direct Search method. This optimization method is chosen in order to ensure a good exploitation of the design variables domain. From the optimization results, it is observed that a unique solution for the vehicle suspensions design is found, being characterized by an operational velocity of the vehicle that increases the original by 9 m/s (32.4 km/h) with respect to the velocity that cancels the *NCA* without exceeding the limits imposed in the standards.

The work presented here was developed considering industrial applications, namely, the homologation of railway vehicles. One particular case where the approach proposed here shows a good potential is the case where an existing vehicle already homologated suffers a minor modification, for example, a change of the track in which it operates. In this case, a dedicated model of the railway vehicle and the track is required. The selection of the track must accomplish the specifications imposed in the standards, namely, the track irregularities must be considered and the track extension must fulfil the requirements. Once the vehicle is homologated for such scenario, this vehicle can operate in any similar track or another track characterized by lower levels of degradation. Afterwards, the optimal vehicle is valid if it suffered minor modifications, namely, if the modifications are in the ranges stablished in the standards, otherwise, experimental tests of the modified vehicle must be performed in order to verify that the proposed modifications leads to vehicle response improvement. In addition, taking into account that a real track is characterized by slopes and curves with different curvatures and cants, the control of the velocity must be achieved as function of the track length. This optimization approach can be adapted for validation if experimental results exist. For example, the objective function can be defined by an absolute difference between the *CV* obtained from the experimental and the numerical results.

In future developments, the optimization tool implemented can be improved by allowing the simulations to be parallelized. In this way, the time that the optimization method takes to converge to a solution can be reduced significantly. The use of the methodology can be generalized by formulation the optimization problem considering multiple objective functions. This approach allows for a compromise between the increase of the velocity and the penalization of the *CV*. Moreover, the domain of the design variables should be defined considering the components characteristics available by the manufactures, leading to a discrete domain, and hence to a limited cases to evaluate.

Acknowledgments This work was supported by Fundação para a Ciência e a Tecnológica (FCT), through the grant with the reference SFRH/BD/96695/2013.

References

[1] Y. Bezin, C. Funfschilling, S. Kraft, and L. Mazzola, "Virtual testing environment tools for railway vehicle certification," *Proceedings of the Institution of Mechanical Engineers, Part F: Journal of Rail and Rapid Transit,* vol. 229, pp. 755-769, August 1, 2015 2015.

[2] O. Polach, A. Böttcher, D. Vannucci, J. Sima, H. Schelle, H. Chollet, *et al.*, "Validation of simulation models in the context of railway vehicle acceptance," *Proceedings of the Institution of Mechanical Engineers, Part F: Journal of Rail and Rapid Transit,* October 28, 2014 2014.

[3] C. Funfschilling, G. Perrin, M. Sebes, Y. Bezin, L. Mazzola, and M.-L. Nguyen-Tajan, "Probabilistic simulation for the certification of railway vehicles," *Proceedings of the Institution of Mechanical Engineers, Part F: Journal of Rail and Rapid Transit,* vol. 229, pp. 770-781, August 1, 2015 2015.

[4] N. Willson, R. Fries, M. Witte, A. Haigermoser, M. Wrang, J. Evans, *et al.*, "Assessment of safety against derailment using simulation and vehicle acceptance tests: a worldwide comparison of state-of-the-art assessment methods," *Vehicle System Dynamics,* vol. 49, pp. 1113-1157, 2011.

[5] UIC 518, "Testing and approval of railway vehicles from the point of view of their dynamic behaviour - Safety - Track fatigue - Running behaviour," ed, 2009.

[6] EN 14363, "Railway applications - Testing for the acceptance of running characteristics of railway vehicles - Testing of running behaviour and stationary tests," ed, 2005, pp. CENELEC European Committee for Electrotechnical Standardization, Brussels, Belgium.

[7] O. Polach and J. Evans, "Simulations of Running Dynamics for Vehicle Acceptance: Application and Validation," *International Journal of Railway Technology,* vol. 2, pp. 59-84 (DOI:10.4203/ijrt.2.4.4), 2013.

[8] L.-O. Jönsson, N. Nilstam, and I. Persson, "Using simulations for approval of railway vehicles: a comparison between measured and simulated track forces," *Vehicle System Dynamics,* vol. 46, pp. 869-881, 2008/09/01 2008.

[9] J. C. Gonçalves and J. C. Ambrósio, "Road Vehicle Modeling Requirements for Optimization of Ride and Handling," *Multibody System Dynamics,* vol. 13, pp. 3-23, 2005/02/01 2005.

[10] J. Gonçalves and J. Ambrósio, "Optimization of Vehicle Suspension Systems for Improved Comfort of Road Vehicles Using Flexible Multibody Dynamics," *Nonlinear Dynamics,* vol. 34, pp. 113-131, 2003.

[11] R. Corradi, S. Melzi, F. Ripamonti, and M. Romani, "Estimation of the Comfort Indexes of a Rail Vehicle at Design Stage," in *ASME 8th Biennial Conference on Engineering Systems Design and Analysis*, 2006, pp. 909-915.

[12] D. Gong, J.-s. Zhou, and W.-j. Sun, "On the resonant vibration of a flexible railway car body and its suppression with a dynamic vibration absorber," *Journal of Vibration and Control,* February 14, 2012 2012.

[13] J. Martínez-Casas, L. Mazzola, L. Baeza, and S. Bruni, "Numerical estimation of stresses in railway axles using a train–track interaction model," *International Journal of Fatigue,* vol. 47, pp. 18-30, 2// 2013.

[14] S. Bruni, J. Vinolas, M. Berg, O. Polach, and S. Stichel, "Modelling of suspension components in a rail vehicle dynamics context," *Vehicle System Dynamics,* vol. 49, pp. 1021-1072, 2011.

[15] B. M. Eickhoff, J. R. Evans, and A. J. Minnis, "A Review of Modelling Methods for Railway Vehicle Suspension Components," *Vehicle System Dynamics,* vol. 24, pp. 469-496, 1995/07/01 1995.

[16] S. Alfi, S. Bruni, and L. Mazzola, "Impact of suspension component modelling on the accuracy of rail vehicle dynamics simulation," in *Procedings of the 11th Mini conference on Vehicle System Dynamics, Identification and Anomalies, Budapest, Hungary*, 2008.

[17] P. E. Nikravesh, *Computer-Aided Analysis of Mechanical Systems*. Englewood Cliffs, New Jersey: Prentice-Hall, 1988.

[18] P. Flores, J. Ambrósio, J. Claro, H. Lankarani, and C. Koshy, "Lubricated Revolute Joints in Rigid Multibody Systems," *Nonlinear Dynamics,* vol. 56, pp. 277-295, 2009.

[19] J. Ambrósio and P. Verissimo, "Improved Bushing Models for General Multibody Systems and Vehicle Dynamics," *Multibody Systems Dynamics,* vol. 22, pp. pp. 341-365, 2009.

[20] J. Pombo and J. Ambrósio, "An Alternative Method to Include Track Irregularities in Railway Vehicle Dynamic Analyses," *Nonlinear Dynamics,* vol. 68, pp. 161-176, 2012.

[21] J. Piotrowski and H. Chollet, "Wheel–rail contact models for vehicle system dynamics including multi-point contact," *Vehicle System Dynamics*, vol. 43, pp. 455-483, 2005/06/01 2005.
[22] K. Knothe, "History of wheel/rail contact mechanics: from Redtenbacher to Kalker," *Vehicle System Dynamics*, vol. 46, pp. 9-26, 2008/02/01 2008.
[23] R. Enblom, "Deterioration mechanisms in the wheel–rail interface with focus on wear prediction: a literature review," *Vehicle System Dynamics*, vol. 47, pp. 661-700, 2009/06/01 2009.
[24] A. Alonso, A. Guiral, and J. G. Giménez, "Wheel-Rail Contact: Theoretical and Experimental Analysis," *International Journal of Railway Technology*, vol. 2, pp. 15-32 (DOI:10.4203/ijrt.2.4.2), 2013.
[25] M. S. Sichani, R. Enblom, and M. Berg, "Non-Elliptic Wheel-Rail Contact Modelling in Vehicle Dynamics Simulation," *International Journal of Railway Technology*, vol. 3, pp. 77-96 (DOI:10.4203/ijrt.3.3.5), 2014.
[26] S. Iwnicki, *Handbook of Railway Vehicle Dynamics*. London, UK: Taylor & Francis, 2006.
[27] J. Pombo, J. Ambrósio, and M. Silva, "A New Wheel-Rail Contact Model for Railway Dynamics," *Vehicle System Dynamics*, vol. 45, pp. 165-189, 2007.
[28] H. M. Lankarani and P. E. Nikravesh, "A Contact Force Model With Hysteresis Damping for Impact Analysis of Multibody Systems," *Journal of Mechanical Design*, vol. 112, pp. 369-376, 1990.
[29] O. Polach, "A Fast Wheel-Rail Forces Calculation Computer Code," *Vehicle System Dynamics*, pp. 728-739, 1999.
[30] J. Pombo and J. Ambrósio, "Application of a Wheel-Rail Contact Model to Railway Dynamics in Small Radius Curved Tracks," *Multibody Systems Dynamics*, vol. 19, pp. 91-114, 2008.
[31] E. Meli and A. Ridolfi, "An innovative wheel–rail contact model for railway vehicles under degraded adhesion conditions," *Multibody System Dynamics*, vol. 33, pp. 285-313, 2015/03/01 2015.
[32] E. Meli, L. Pugi, and A. Ridolfi, "An innovative degraded adhesion model for multibody applications in the railway field," *Multibody System Dynamics*, vol. 32, pp. 133-157, 2014/08/01 2014.
[33] B. Allota, R. Conti, E. Meli, L. Pugi, and A. Ridolfi, "Railway Vehicle Dynamics under Degraded Adhesion Conditions: An Innovative HIL Architecture for Braking Tests on Full-Scale Roller-Rigs," *International Journal of Railway Technology*, vol. 2, pp. 21-53 (DOI:10.4203/ijrt.2.3.2), 2013.
[34] M. Sebès, L. Chevalier, J.-B. Ayasse, and H. Chollet, "A fast-simplified wheel–rail contact model consistent with perfect plastic materials," *Vehicle System Dynamics*, vol. 50, pp. 1453-1471, 2012/09/01 2012.
[35] M. Sebès, H. Chollet, J.-B. Ayasse, and L. Chevalier, "A multi-Hertzian contact model considering plasticity," *Wear*, vol. 314, pp. 118-124, 2014.
[36] M. Ignesti, A. Innocenti, L. Marini, E. Meli, and A. Rindi, "Development of a model for the simultaneous analysis of wheel and rail wear in railway systems," *Multibody System Dynamics*, vol. 31, pp. 191-240, 2014/02/01 2014.
[37] A. Ekberg, B. Åkesson, and E. Kabo, "Wheel/rail rolling contact fatigue – Probe, predict, prevent," *Wear*, vol. 314, pp. 2-12, 2014.
[38] J. Ding, F. Li, Y. Huang, S. Sun, and L. Zhang, "Application of the semi-Hertzian method to the prediction of wheel wear in heavy haul freight car," *Wear*, vol. 314, pp. 104-110, 2014.
[39] H. Sugiyama, M. Yada, Y. H., J. Kurihara, H. Ohbayashi, Y. Shimokawa, *et al.*, "Wheel and Rail Profile Wear on Small Radius Curved Tracks and its Effect on Derailment Coefficients: Measurement and Simulation," *International Journal of Railway Technology*, vol. 2, pp. 85-98 (DOI:10.4203/ijrt.2.4.5), 2013.
[40] O. Polach and A. Böttcher, "A new approach to define criteria for rail vehicle model validation," *Vehicle System Dynamics*, vol. 52, pp. 125-141, 2014.
[41] B. Suarez, J. M. Mera, M. L. Martinez, and J. A. Chover, "Assessment of the influence of the elastic properties of rail vehicle suspensions on safety, ride quality and track fatigue," *Vehicle System Dynamics*, vol. 51, pp. 280-300, 2013/02/01 2012.
[42] B. Suarez, J. Felez, J. Maroto, and P. Rodriguez, "Sensitivity analysis to assess the influence of the inertial properties of railway vehicle bodies on the vehicle's dynamic behaviour," *Vehicle System Dynamics*, vol. 51, pp. 251-279, 2013/02/01 2012.
[43] B. Suarez, J. Felez, J. Antonio Lozano, and P. Rodriguez, "Influence of the track quality and of the properties of the wheel–rail rolling contact on vehicle dynamics," *Vehicle System Dynamics*, vol. 51, pp. 301-320, 2013/02/01 2012.
[44] H. Magalhães, J. Ambrósio, and J. Pombo, "Railway vehicle modelling for the vehicle–track interaction compatibility analysis," *Proceedings of the Institution of Mechanical Engineers, Part K: Journal of Multi-body Dynamics*, 2015.
[45] J. S. Arora, *Introduction to Optimum Design*. Boston: Academic Press, 2012.
[46] É. Walter, *Numerical Methods and Optimization: A Consumer Guide*: Springer International Publishing, 2014.

[47] K. Deb, S. Agrawal, A. Pratap, and T. Meyarivan, "A Fast Elitist Non-dominated Sorting Genetic Algorithm for Multi-objective Optimization: NSGA-II," in *Parallel Problem Solving from Nature PPSN VI*. vol. 1917, M. Schoenauer, K. Deb, G. Rudolph, X. Yao, E. Lutton, J. Merelo, *et al.*, Eds., ed: Springer Berlin Heidelberg, 2000, pp. 849-858.
[48] M. Carvalho, J. Ambrósio, and P. Eberhard, "Identification of validated multibody vehicle models for crash analysis using a hybrid optimization procedure," *Structural and Multidisciplinary Optimization,* vol. 44, pp. 85-97, 2011/07/01 2011.
[49] P. Eberhard, F. Dignath, and L. Kübler, "Parallel Evolutionary Optimization of Multibody Systems with Application to Railway Dynamics," *Multibody System Dynamics,* vol. 9, pp. 143-164, 2003/03/01 2003.
[50] S. N. Sivanandam and S. N. Deepa, *Introduction to Genetic Algorithms*: Springer Berlin Heidelberg, 2007.
[51] S. Kirkpatrick, C. D. Gelatt, and M. P. Vecchi, "Optimization by Simulated Annealing," *Science,* vol. 220, pp. 671-680, May 13, 1983 1983.
[52] V. Gazi and K. M. Passino, *Swarm Stability and Optimization*: Springer Berlin Heidelberg, 2011.
[53] T. J. Aird and J. R. Rice, "Systematic Search in High Dimensional Sets," *SIAM Journal on Numerical Analysis,* vol. 14, pp. 296-312, 1977.
[54] R. H. Myers, D. C. Montgomery, and C. M. Anderson-Cook, *Response Surface Methodology: Process and Product Optimization Using Designed Experiments*: Wiley, 2009.
[55] A. L. Custódio and J. F. A. Madeira, "GLODS: Global and Local Optimization using Direct Search," *Journal of Global Optimization,* pp. 1-28, 2014/08/13 2014.
[56] J. Pombo, "A Multibody Methodology for Railway Dynamics Applications," PhD Dissertation, IDMEC/Department of Mechanical Engineering, Instituto Superior Técnico, Lisbon, Portugal, 2004.
[57] Y. He and J. McPhee, "Optimization of the Lateral Stability of Rail Vehicles," *Vehicle System Dynamics,* vol. 38, pp. 361-390, 2002.
[58] L. Mazzola and S. Bruni, "Effect of suspension parameter uncertainty on the dynamic behaviour of railway vehicles," in *Applied Mechanics and Materials*, 2012, pp. 177-185.
[59] C. W. Gear, "Simultaneous Numerical Solution of Differential-Algebraic Equations," *IEEE Transactions on Circuit Theory,* vol. 18, pp. 89-95, 1971.
[60] UIC 861-2, "Profiles Unifiés de Rails à rails-aiguilles adptés aux profils de rails UIC 54 et 60 kg/m," ed, 1989.
[61] J. J. Kalker, *Three-Dimensional Elastic Bodies in Rolling Contact*. Dordrecht, The Netherlands: Kluwer Academic Publishers, 1990.
[62] Z. Y. Shen, J. K. Hedrick, and J. A. Elkins, "A Comparison of Alternative Creep Force Models for Rail Vehicle Dynamic Analysis," in *8th IAVSD Symposium on Dynamics of Vehicles on Road and Tracks*, Cambridge, Massachussetts, 1983, pp. 591-605.
[63] J. Pombo, "Application of a Computational Tool to Study the Influence of Worn Wheels on Railway Vehicle Dynamics," *Journal of Software Engineering and Applications,* vol. 5, pp. 51-61, 2012.

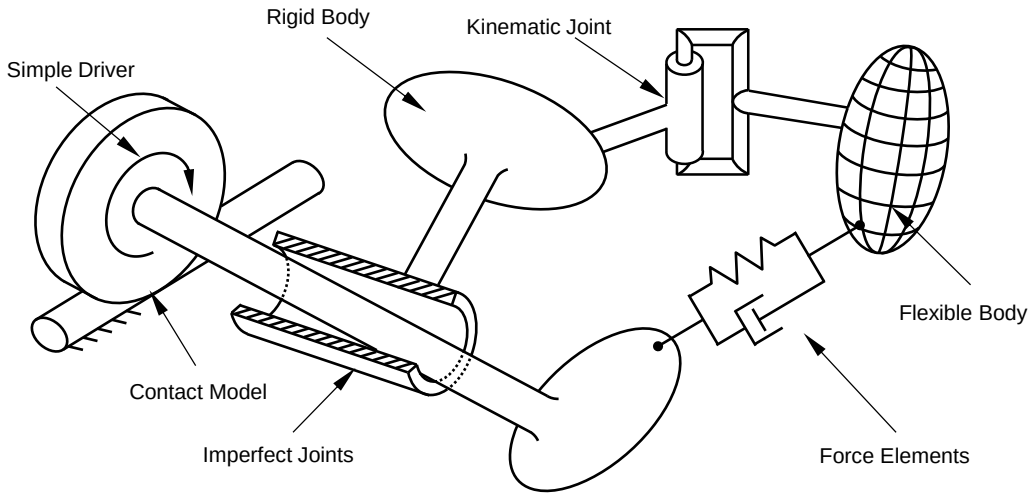

Figure 1: Generic Multibody Model

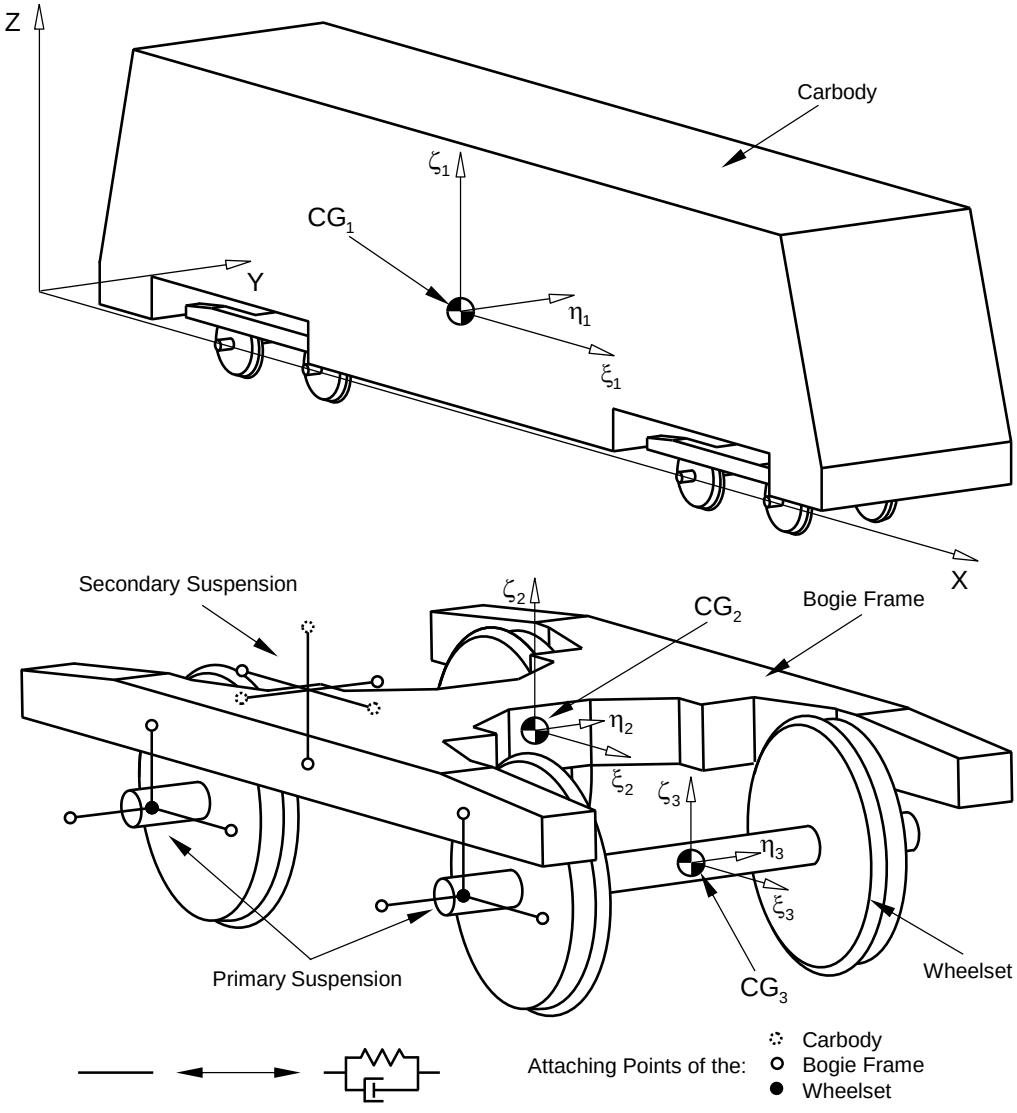

Figure 2: Multibody model of the railway vehicle

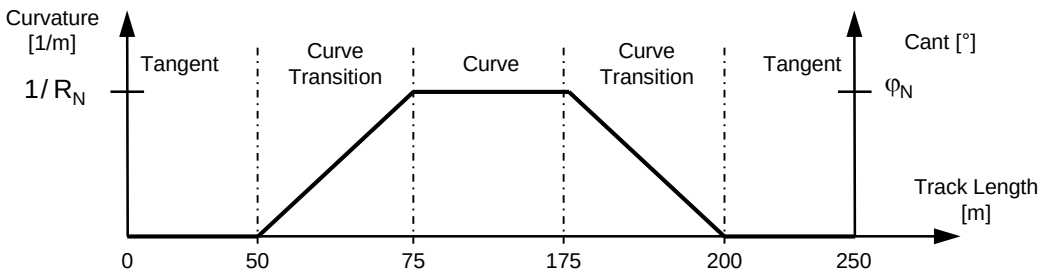

Figure 3: Curvature (*1/R*) and cant angle φ as function of the track length

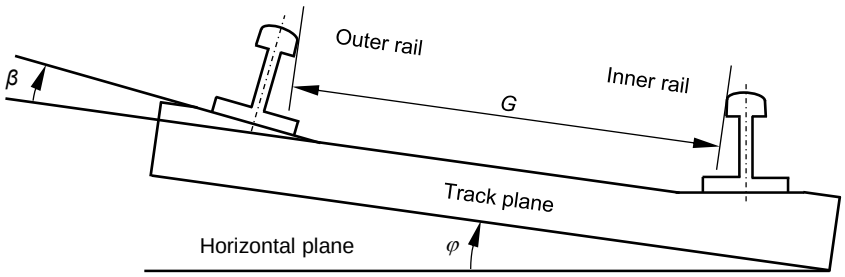

Figure 4: Gauge (*G*), cant angle (φ) and rail cant (β)

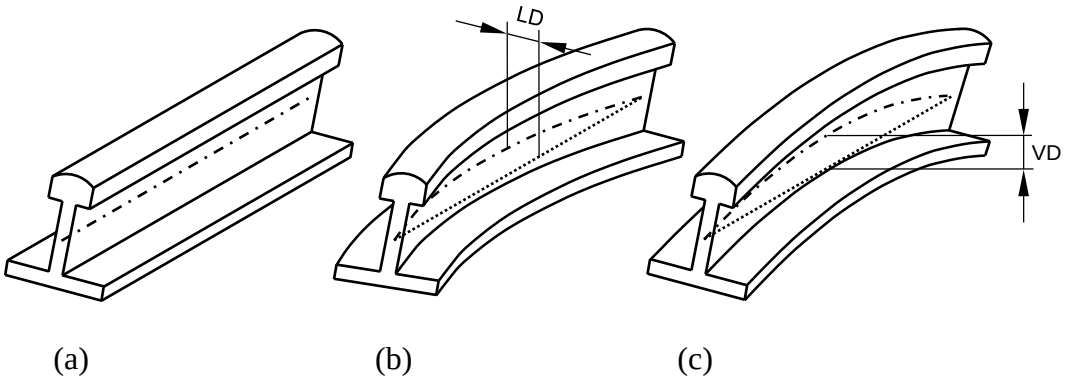

Figure 5: (a) Perfect rail, (b) rail with lateral deviation and (c) rail with vertical deviation

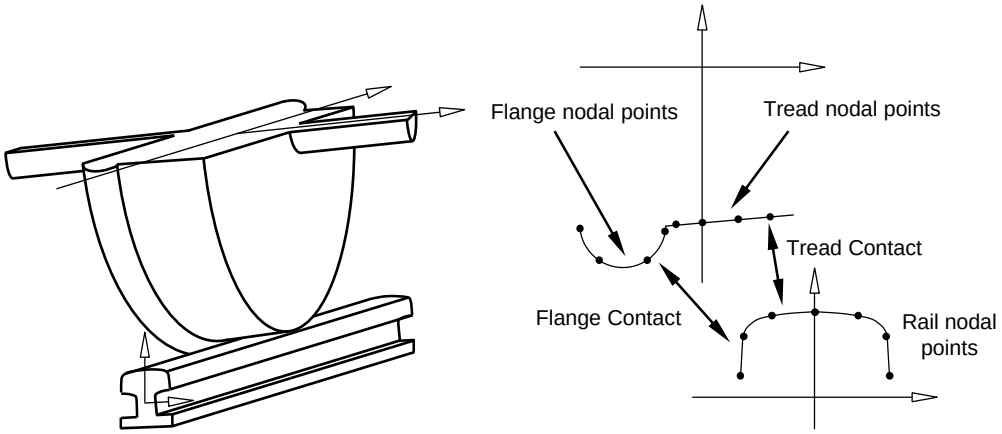

Figure 6: Wheel and rail surfaces

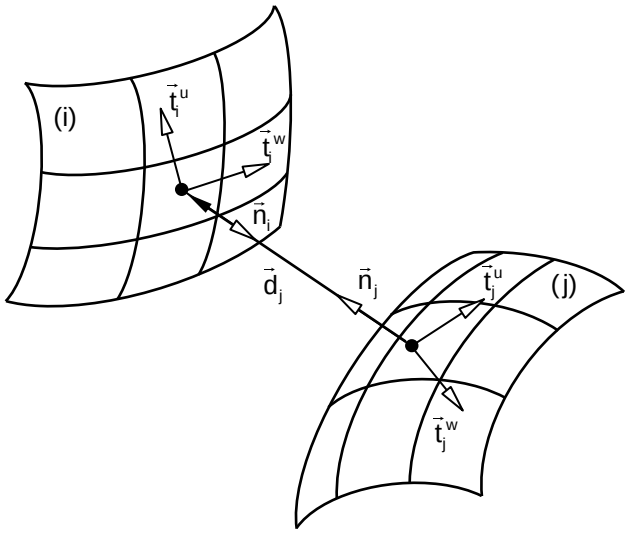

Figure 7: Contact detection between two surfaces

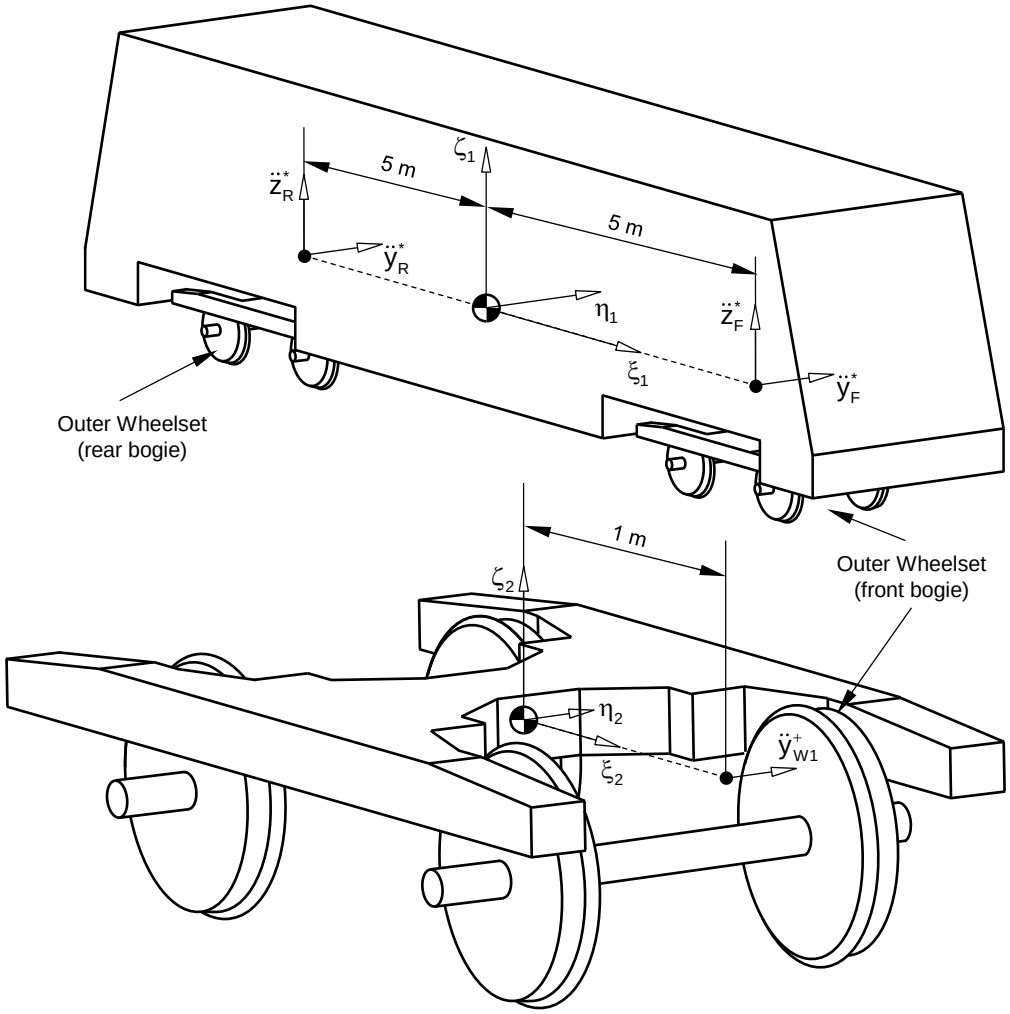

Figure 8: Points of the bodies in which the accelerations $\ddot{y}^{+}_{W1}$, $\ddot{y}^{+}_{W4}$, $\ddot{y}^{*}_{F}$, $\ddot{y}^{*}_{R}$, $\ddot{z}^{*}_{F}$ and $\ddot{z}^{*}_{R}$ are measured for homologation purposes, according to the standards [5, 6]

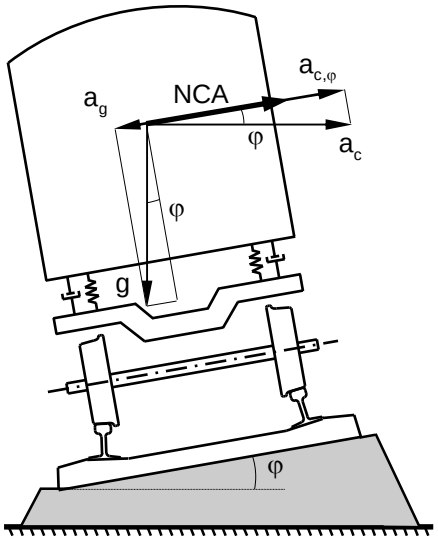

Figure 9: Non-Compensated Acceleration (*NCA*)

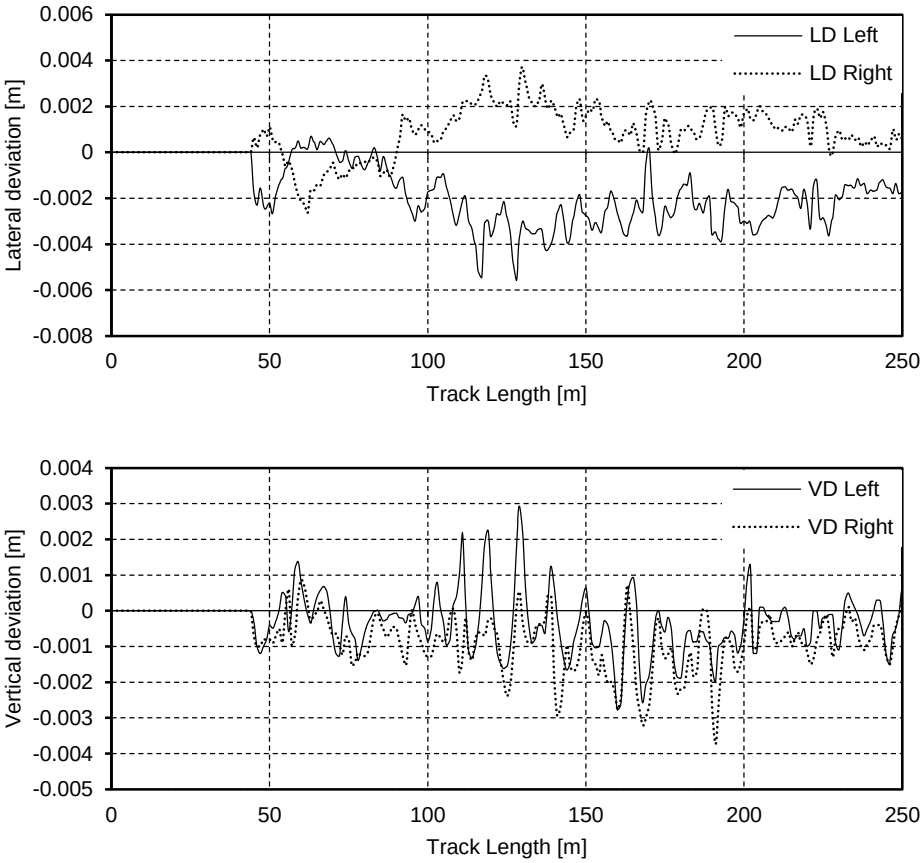

Figure 10: Lateral (top) and vertical (bottom) deviations of the left and right rails

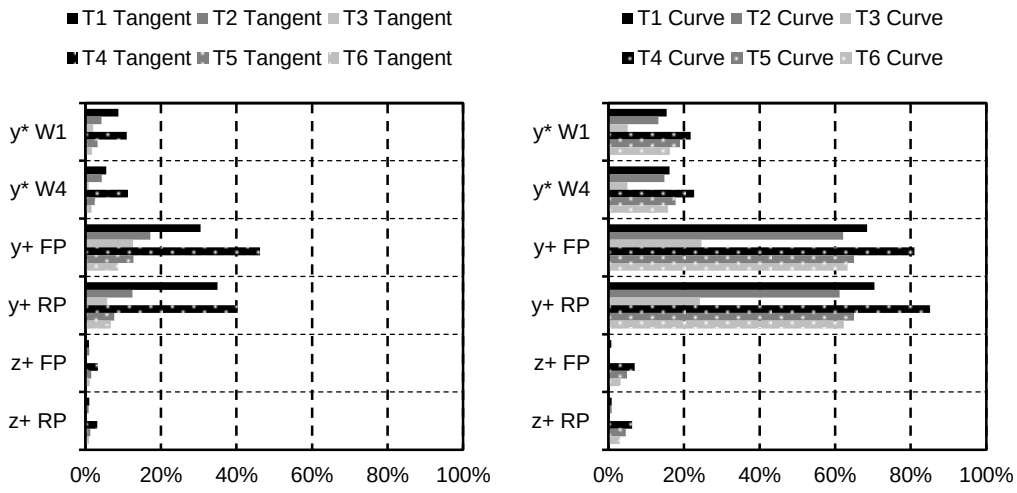

Figure 11: *CV* related to running safety of simulations of the six scenarios

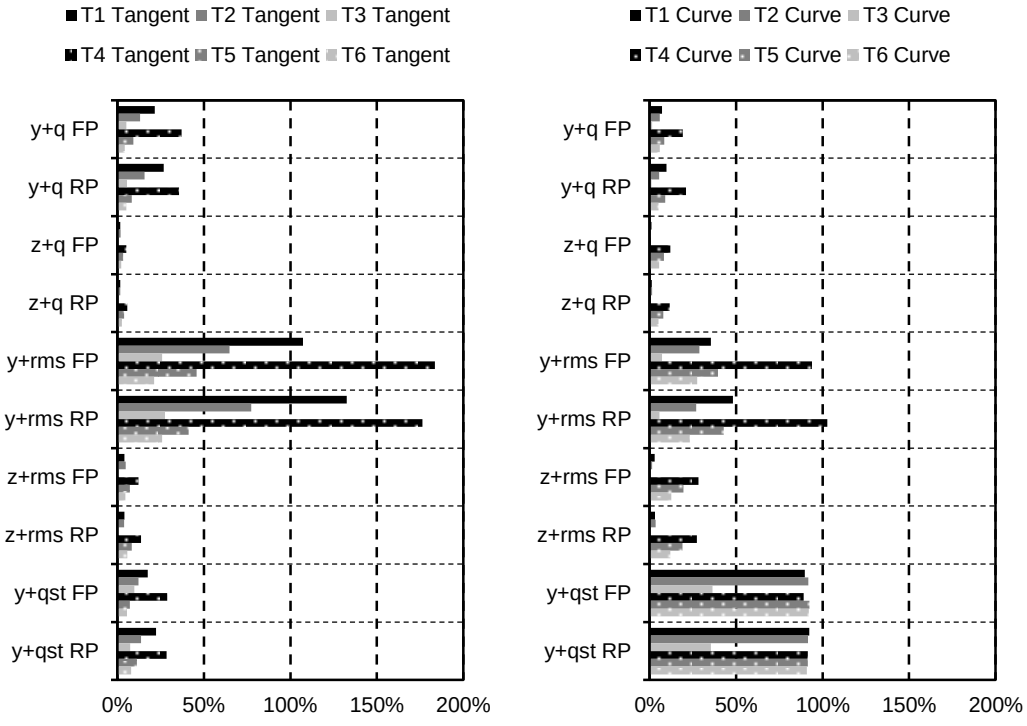

Figure 12: *CV* related to ride characteristics of simulations of the six scenarios

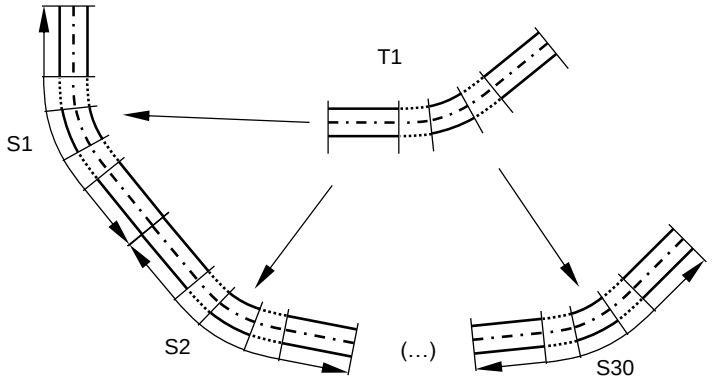

Figure 13: Extended track, used for virtual homologation testing, made of a series of 30 railway segments described in Table 4 with a geometry described in Figure 3

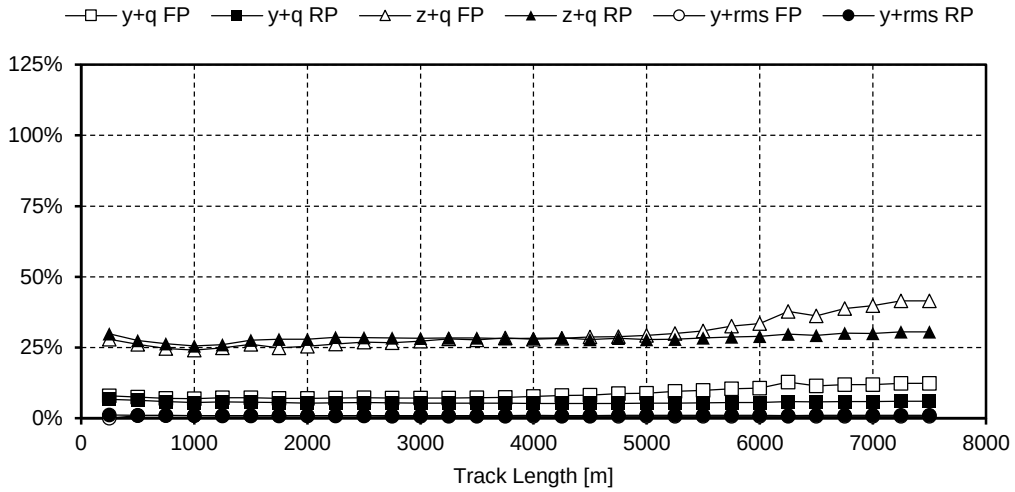

Figure 14: CV^t related to running safety as function of track length

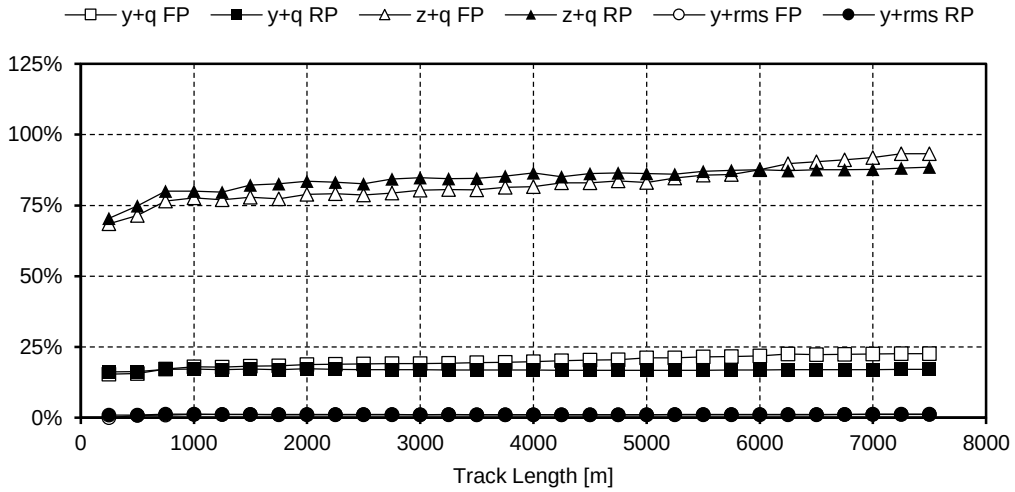

Figure 15: CV^c related to running safety as function of track length

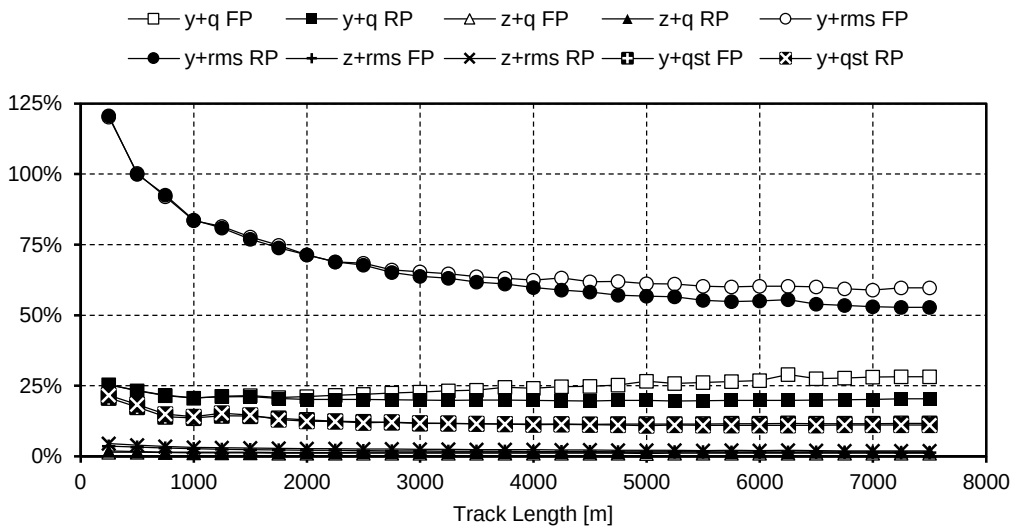

Figure 16: CV^t related to ride characteristics as function of track length

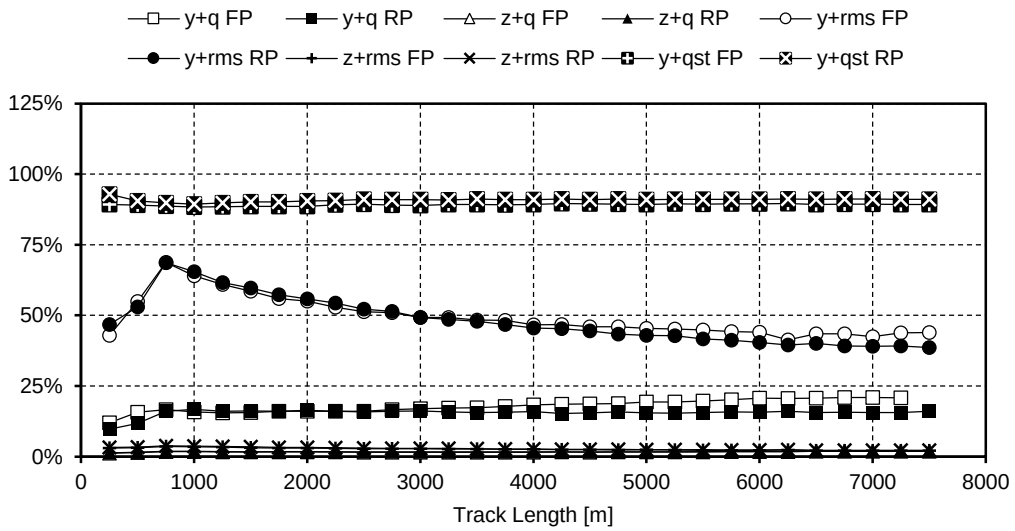

Figure 17: CV^c related to ride characteristics as function of track length

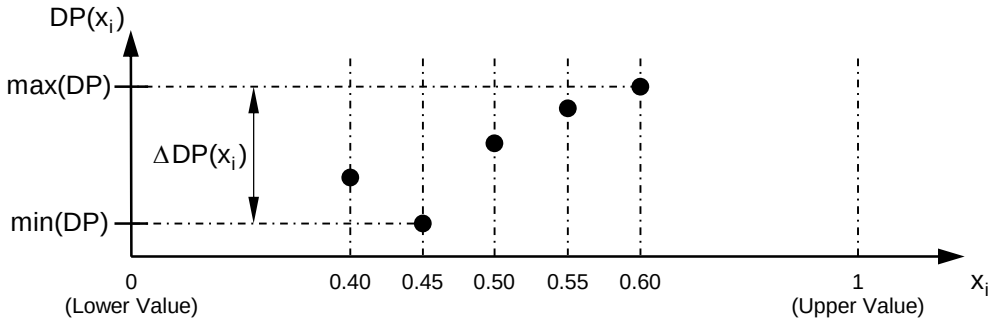

Figure 18: *DP* variation when potential design variables are varied

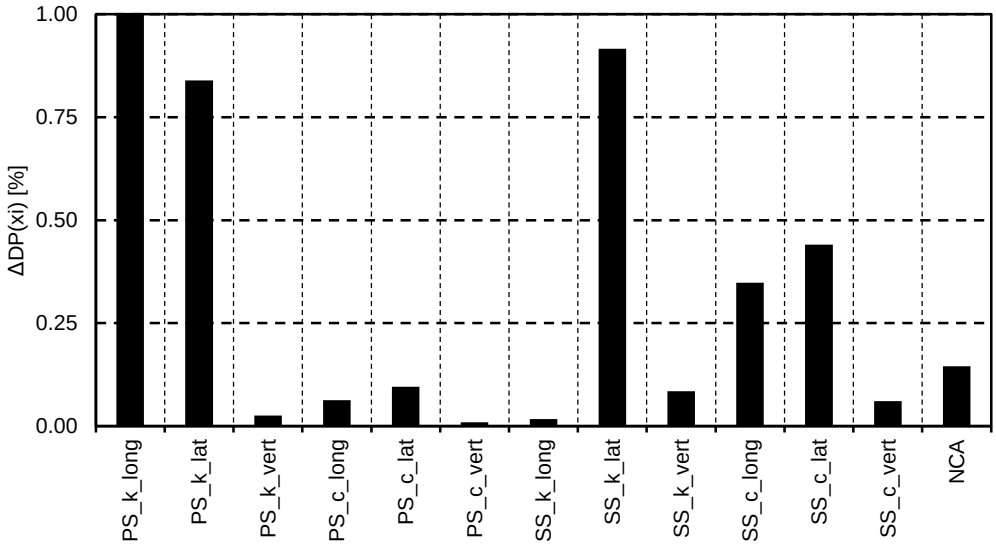

Figure 19: *ΔDP* of each potential design variable

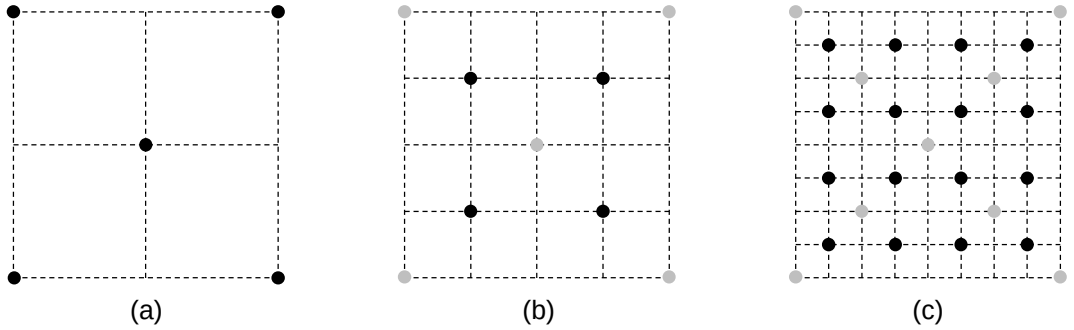

Figure 20: Search step that generate starting points using 2^n-centre strategy of three iterations

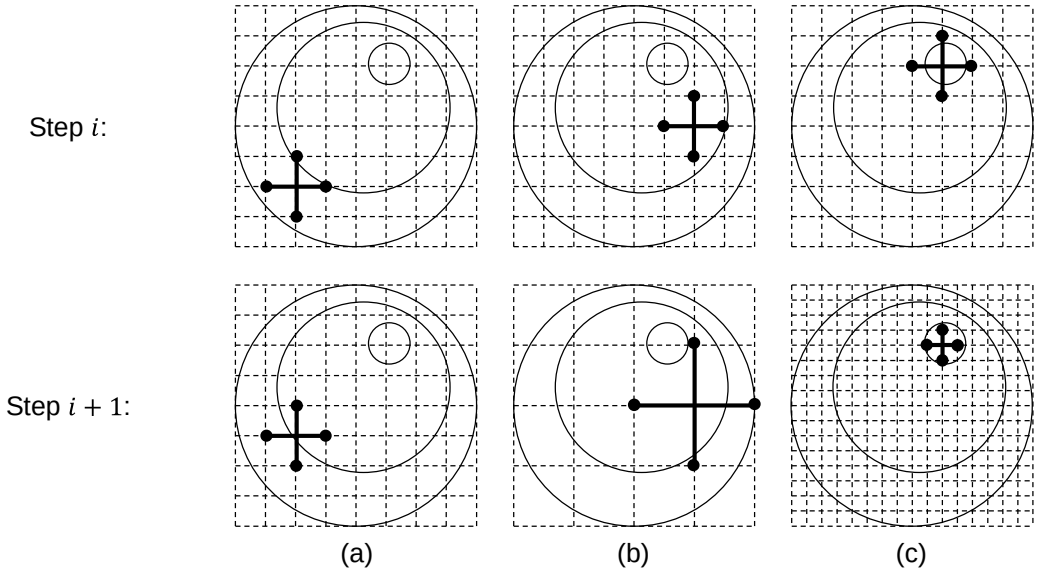

Figure 21: Poll method progression in two consecutive steps: when success occurs and (a) the mesh size is kept equal or (b) the mesh size is increased and (c) when success does not occur and the mesh size is reduced.

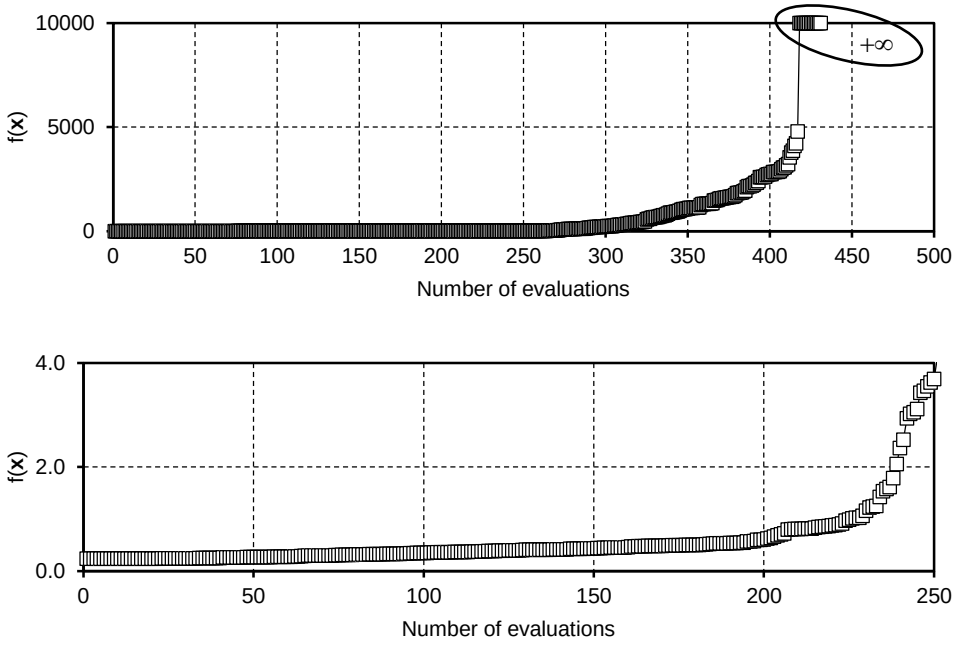

Figure 22: Cost function, $f(\mathbf{x})$, for the 431 point in the top figure. The best 250 points sorted in ascending order are shown in the bottom figure

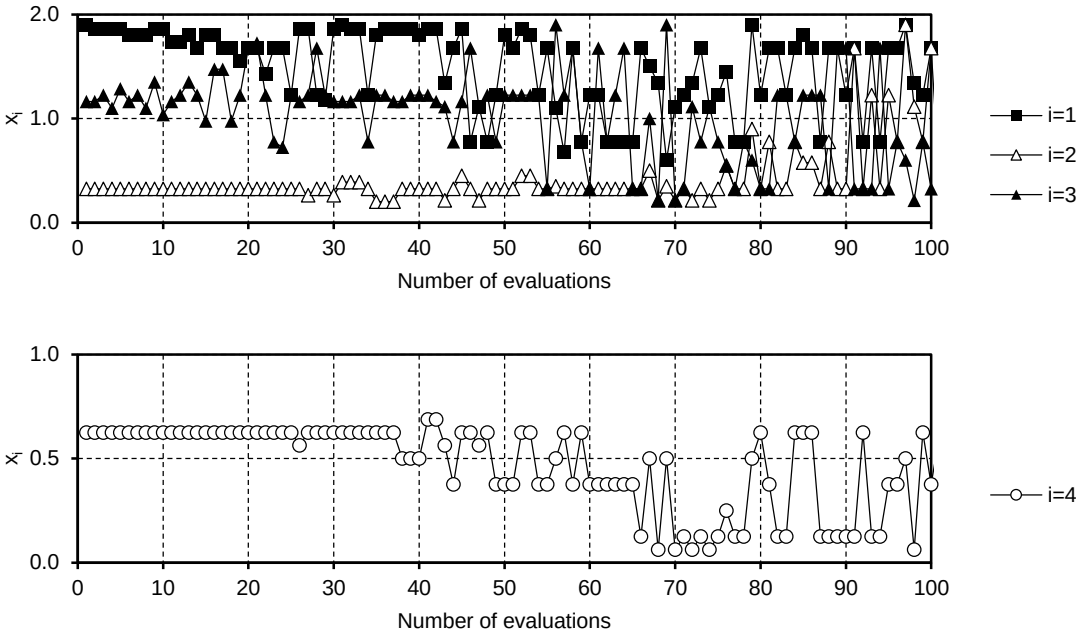

Figure 23: Design variables x_1, x_2 and x_3 (top) and x_4 (bottom) of the 100 best points according to the ascending order of function cost $f(\mathbf{x})$

ID	Rigid Body	Centre of Mass (m) *(X/Y/Z)*	Mass (Kg)	Moment of Inertia (Kg/m^2) *ξξ/ηη/ζζ*
1	Carbody	(7.000 / 0.002 / 1.500)	20000	20000 / 200000 / 200000
2	Front Bogie Frame	(12.000 / 0.002 / 0.600)	3000	3000 / 3000 / 3000
3	Front Wheelset (W1)	(13.000 / 0.002 / 0.450)	1000	1000 / 100 / 1000
4	Rear Wheelset (W2)	(11.000 / 0.002 / 0.450)	1000	1000 / 100 / 1000
5	Rear Bogie Frame	(2.000 / 0.002 / 0.600)	3000	3000 / 3000 / 3000
6	Front Wheelset (W3)	(3.000 / 0.002 / 0.450)	1000	1000 / 100 / 1000
7	Rear Wheelset (W4)	(1.000 / 0.002 / 0.450)	1000	1000 / 100 / 1000

Table 1: Centre of gravity (*CG*) and mass properties the rigid bodies

Force Element	Direction	Bodies *i*	Bodies *j*	*k* (kN/m)	L_0 (m)	*c* (kNs/m)	Attach. Pts: P_i, P_j (m) $(\xi_i,\eta_i,\zeta_i)^P$ and $(\xi_j,\eta_j,\zeta_j)^P$
Primary Suspension (Left wheel of the leading wheelset)	Longitudinal	2	3	1000	0.200	10	(1.200, 0.5275, -0.155) (0.000, 0.5275, 0.000)
	Lateral	2	3	1000	0.200	10	(1.000, 0.6275, -0.155) (0.000, 0. 4275, 0.000)
	Vertical	2	3	500	0.364	50	(1.000, 0.5275, 0.145) (0.000, 0. 5275, 0.000)
Secondary Suspension (Left side of the leading bogie)	Longitudinal	1	2	1000	0.200	500	(5.100, 0.5275, -0.650) (-0.100, 0.5275, 0.250)
	Lateral	1	2	1000	0.200	50	(5.000, 0.6275, 0.650) (0.000, 0.4275, 0.250)
	Vertical	1	2	200	0.745	50	(5.000, 0.5275, -0.400) (0.000, 0.5275, 0.000)

Table 2: Linear force elements used to model the suspension system

Accelerations	Filter	Statistical quantity	K	Characteristics Values (CV)
$\ddot{y}^+_{W1}$ $\ddot{y}^+_{W4}$	Low-pass filter: [0-10] Hz	$F_1 = 0.15\%$; $F_2 = 99.85\%$	3.0	$\left(\ddot{y}^+_s\right)_{W1}$ $\left(\ddot{y}^+_s\right)_{W4}$
$\ddot{y}^*_F$ $\ddot{y}^*_R$	Low-pass filter: [0-6] Hz	$F_1 = 0.15\%$; $F_2 = 99.85\%$	3.0	$\left(\ddot{y}^*_s\right)_F$ $\left(\ddot{y}^*_s\right)_R$
$\ddot{z}^*_F$ $\ddot{z}^*_R$	Band-pass filter: [0.4-4] Hz	$F_1 = 0.15\%$; $F_2 = 99.85\%$	3.0	$\left(\ddot{z}^*_s\right)_F$ $\left(\ddot{z}^*_s\right)_R$
$\ddot{y}^*_F$ $\ddot{y}^*_R$ $\ddot{z}^*_F$ $\ddot{z}^*_R$	Band-pass filter: [0.4-10] Hz	$F_1 = 0.15\%$; $F_2 = 99.85\%$	2.2	$\left(\ddot{y}^*_q\right)_F$ $\left(\ddot{y}^*_q\right)_R$ $\left(\ddot{z}^*_q\right)_F$ $\left(\ddot{z}^*_q\right)_R$
$\ddot{y}^*_F$ $\ddot{y}^*_R$ $\ddot{z}^*_F$ $\ddot{z}^*_R$	Band-pass filter: [0.4-10] Hz	Root mean square	2.2	$\left(\ddot{y}^*_{rms}\right)_F$ $\left(\ddot{y}^*_{rms}\right)_R$ $\left(\ddot{z}^*_{rms}\right)_F$ $\left(\ddot{z}^*_{rms}\right)_R$
$\ddot{y}^*_F$ $\ddot{y}^*_R$	Low-pass filter: [0-20] Hz	$F_0 = 50\%$	0.0	$\left(\ddot{y}^*_{qst}\right)_F$ $\left(\ddot{y}^*_{qst}\right)_R$

Table 3: Post-Processing settings defined in standards [5, 6], being the acceleration measured at the locations specified in Figure 8

Simulation	Radius [m]	Cant angle [°]	Irregularities
T1	1000	5	No
T2	500	5	No
T3	200	5	No
T4	1000	5	Yes
T5	500	5	Yes
T6	200	5	Yes

Table 4: Characteristics for the track used in simulations performed in this work

i		$CV_{i,\,j=1}$	$CV_{i,\,j=2}$	$CV_{i,\,j=1}^{\lim}$	$CV_{i,\,j=2}^{\lim}$	$w_{i,\,j=1}$	$w_{i,\,j=2}$
1	$\left(\ddot{y}_s^+\right)_{W1}$	0.797	2.132	11.4	11.4	0.104	0.093
2	$\left(\ddot{y}_s^+\right)_{W4}$	0.604	1.965	11.4	11.4	0.079	0.086
3	$\left(\ddot{y}_s^*\right)_F$	0.762	2.050	3.0	2.6	0.378	0.393
4	$\left(\ddot{y}_s^*\right)_R$	0.836	2.171	3.0	2.6	0.415	0.417
5	$\left(\ddot{z}_s^*\right)_F$	0.037	0.053	5.0	5.0	0.011	0.005
6	$\left(\ddot{z}_s^*\right)_R$	0.045	0.056	5.0	5.0	0.013	0.006
7	$\left(\ddot{y}_q^*\right)_F$	0.531	0.402	2.5	2.5	0.098	0.048
8	$\left(\ddot{y}_q^*\right)_R$	0.504	0.411	2.5	2.5	0.093	0.049
9	$\left(\ddot{z}_q^*\right)_F$	0.028	0.041	2.5	2.5	0.005	0.005
10	$\left(\ddot{z}_q^*\right)_R$	0.034	0.043	2.5	2.5	0.006	0.005
11	$\left(\ddot{y}_{rms}^*\right)_F$	0.357	0.275	0.5	0.5	0.329	0.166
12	$\left(\ddot{y}_{rms}^*\right)_R$	0.357	0.279	0.5	0.5	0.329	0.168
13	$\left(\ddot{z}_{rms}^*\right)_F$	0.022	0.030	1.0	1.0	0.010	0.009
14	$\left(\ddot{z}_{rms}^*\right)_R$	0.027	0.032	1.0	1.0	0.013	0.010
15	$\left(\ddot{y}_{qst}^*\right)_F$	0.193	1.329	1.5	1.5	0.059	0.267
16	$\left(\ddot{y}_{qst}^*\right)_R$	0.186	1.358	1.5	1.5	0.057	0.273

Table 5: *CV* for the original design and their respective limits and weights

Potential design variables			Lower bound	Original value	Upper bound
PS	k	longitudinal	$\chi k_{PS,long}^0$	$k_{PS,long}^0$	$(1-\chi)k_{PS,long}^0$
		lateral	$\chi k_{PS,lat}^0$	$k_{PS,lat}^0$	$(1-\chi)k_{PS,lat}^0$
		vertical	$\chi k_{PS,vert}^0$	$k_{PS,vert}^0$	$(1-\chi)k_{PS,vert}^0$
	c	longitudinal	$\chi c_{PS,long}^0$	$c_{PS,long}^0$	$(1-\chi)c_{PS,long}^0$
		lateral	$\chi c_{PS,lat}^0$	$c_{PS,lat}^0$	$(1-\chi)c_{PS,lat}^0$
		vertical	$\chi c_{PS,vert}^0$	$c_{PS,vert}^0$	$(1-\chi)c_{PS,vert}^0$
SS	k	longitudinal	$\chi k_{SS,long}^0$	$k_{SS,long}^0$	$(1-\chi)k_{SS,long}^0$
		lateral	$\chi k_{SS,lat}^0$	$k_{SS,lat}^0$	$(1-\chi)k_{SS,lat}^0$
		vertical	$\chi k_{SS,vert}^0$	$k_{SS,vert}^0$	$(1-\chi)k_{SS,vert}^0$
	c	longitudinal	$\chi c_{SS,long}^0$	$c_{SS,long}^0$	$(1-\chi)c_{SS,long}^0$
		lateral	$\chi c_{SS,lat}^0$	$c_{SS,lat}^0$	$(1-\chi)c_{SS,lat}^0$
		vertical	$\chi c_{SS,vert}^0$	$c_{SS,vert}^0$	$(1-\chi)c_{SS,vert}^0$
NCA			0	0.5	1

Table 6: Definition of the upper and lower bound of the design variables

i	Design variables	Lower bound	Upper bound
x_1	$k_{PS,long}$		
x_2	$k_{PS,lat}$	0.1×10^6 N/m	1.9×10^6 N/m
x_3	$k_{SS,lat}$		
x_4	*NCA*	0 m/s^2	1 m/s^2

Table 7: Design variables and respective bounds

Parameters	Initial	Optimal	Original
$k_{PS,long}$	1 x 10^6 N/m	1.893 10^6 N/m	1 x 10^6 N/m
$k_{PS,lat}$	1 x 10^6 N/m	0.325 10^6 N/m	1 x 10^6 N/m
$k_{SS,lat}$	1 x 10^6 N/m	1.163 10^6 N/m	1 x 10^6 N/m
NCA	0.5 m/s^2	0.625 m/s^2	0.0 m/s^2
Velocity	36.88 m/s	38.54 m/s	29.30 m/s
$f(\mathbf{x})$	0.446	0.237	104.202
Number of evaluation	154	1	-

Table 8: Initial, optimal and original designs of the railway vehicle